Present and projected sensitivities of Dark Matter direct detection experiments to effective WIMP-nucleus couplings

Stefano Scopel

in collaboration with Sunghyun Kang, G. Tomar, J.H. Yoon

서강대학교
SOGANG UNIVERSITY

NDM 2018

6th Symposium on Neutrinos and Dark Matter in Nuclear Physics 2018

2018. 6. 29 (Fri) – 7. 4 (Wed) | IBS HQ, Daejeon, Korea

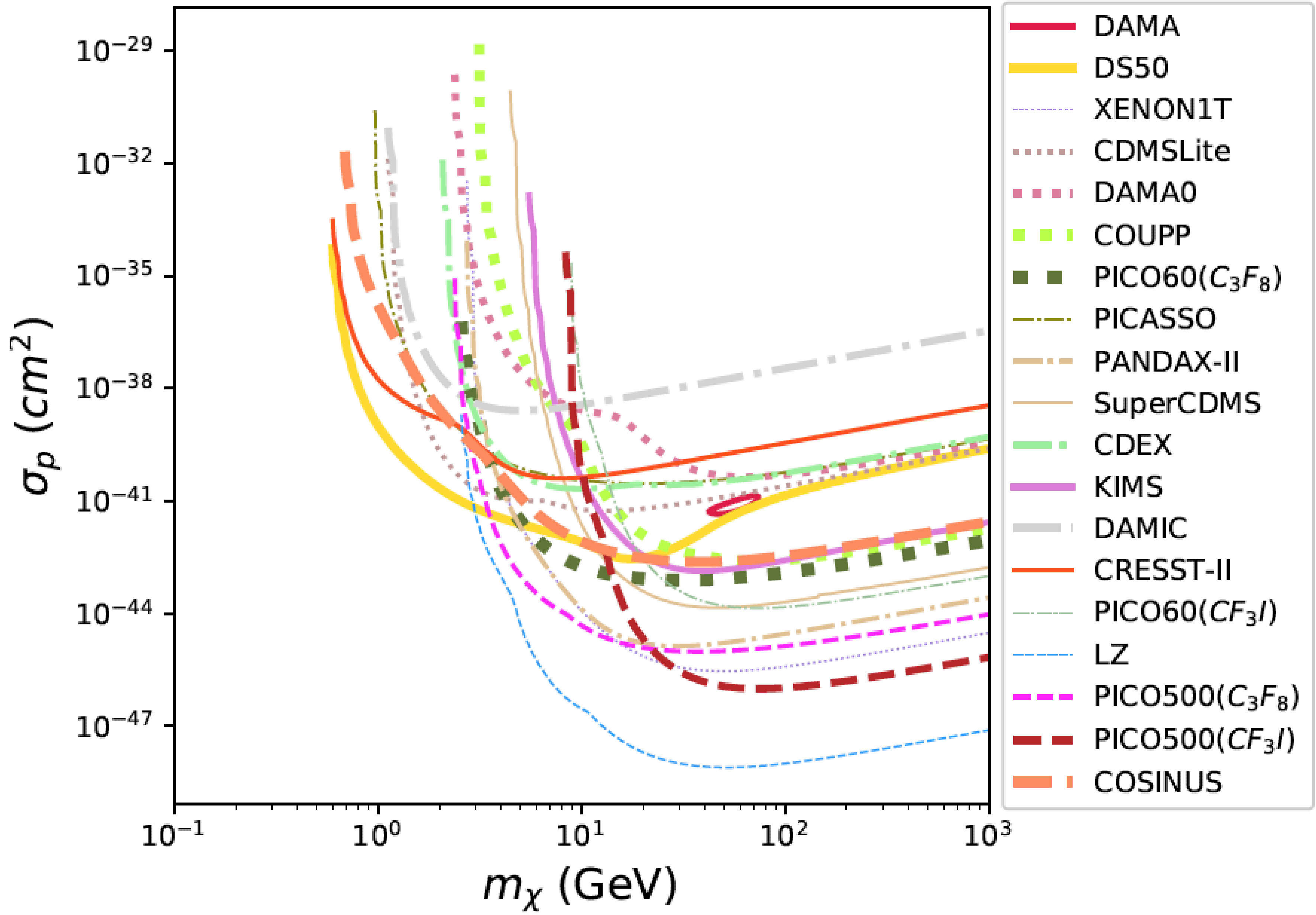

DAMA
DS50
XENON1T
CDMSLite
DAMA0
COUPP
PICO60(C_3F_8)
PICASSO
PANDAX-II
SuperCDMS
CDEX
KIMS
DAMIC
CRESST-II
PICO60(CF_3I)
LZ
PICO500(C_3F_8)
PICO500(CF_3I)
COSINUS
σ_p (cm^2)
m_χ (GeV)
10^{-29}
10^{-32}
10^{-35}
10^{-38}
10^{-41}
10^{-44}
10^{-47}
10^{-1}
10^{0}
10^{1}
10^{2}
10^{3}

N.B.: theoretical predictions for the WIMP direct detection rate depend on two main ingredients:

1) a scaling law for the cross section, in order to compare experiments using different targets

   Traditionally spin-independent cross section (proportional to (atomic mass number)^2) or spin-dependent cross section (proportional to the product $\boldsymbol{S}_{WIMP} \cdot \boldsymbol{S}_{nucleus}$ *) is assumed*

2) a model for the velocity distribution of WIMPs

   Traditionally a Maxwellian distribution is assumed

We focus on the issue of the scaling law, assuming for the WIMP velocity distribution a standard Maxwellian

$$\eta(v_{min}, t) = \int_{v_{min}}^{\infty} \frac{f(v)}{v} dv = \eta_0(v_{min}) + \eta_1(v_{min}) \cos\omega(t - t_0)$$

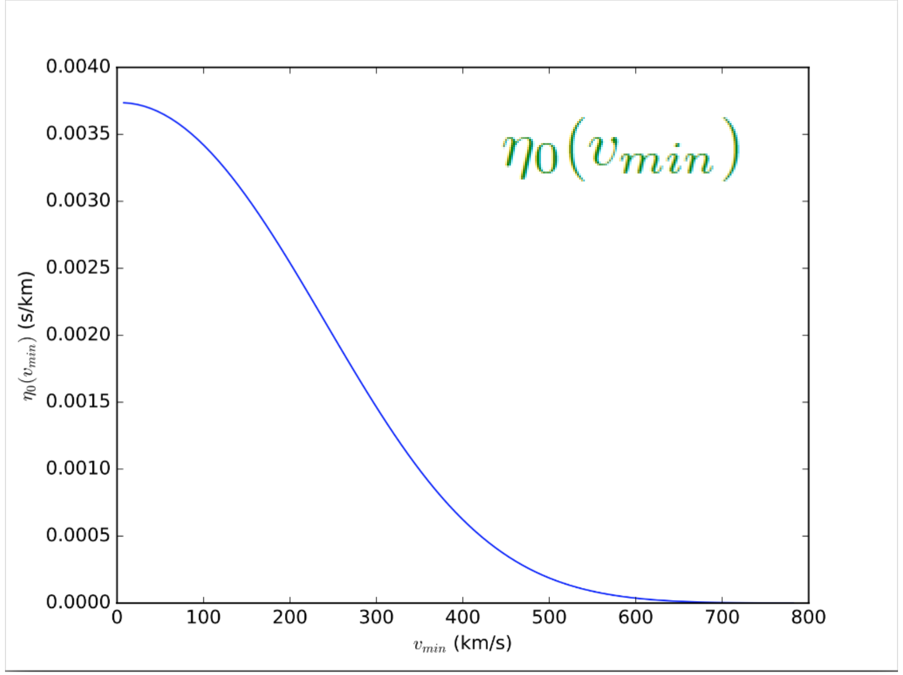

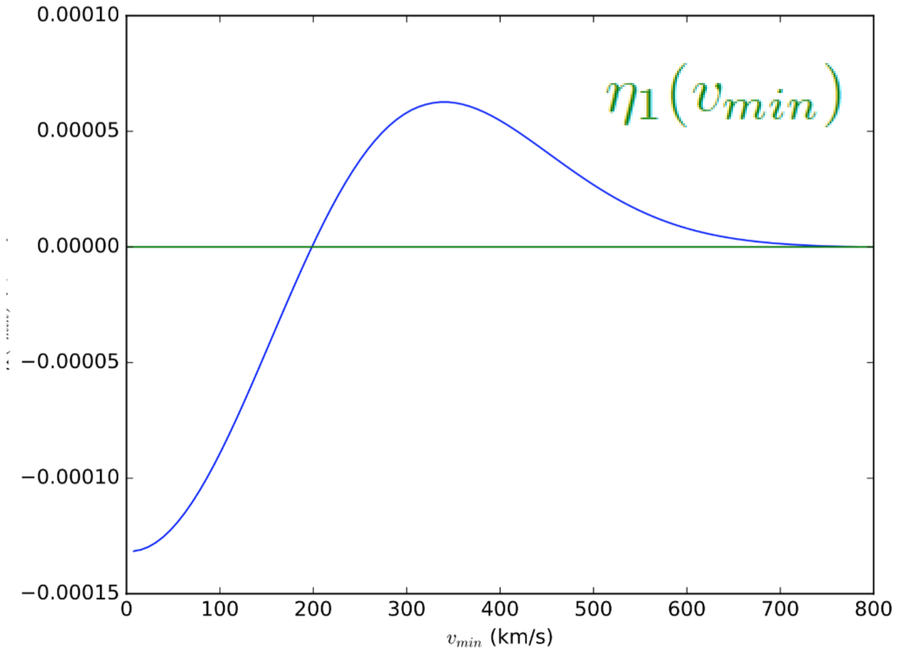

Most general approach: consider all possible NR couplings, including those depending on velocity and momentum

$$\mathcal{H} = \sum_i \left(c_i^0 + c_i^1 \tau_3\right) \mathcal{O}_i$$

τ_3=nuclear isospin operator, i.e.

$$c_i^{\mathrm{p}} = (c_i^0 + c_i^1)/2 \qquad \text{(proton)}$$

$$c_i^{\mathrm{n}} = (c_i^0 - c_i^1)/2 \qquad \text{(neutron)}$$

(if $c_i^p = c_i^n \rightarrow c_i^1=0$)

N.R. operators O_i guaranteed to be Hermitian if built out of the following four 3-vectors:

$$i\frac{\vec{q}}{m_N}, \quad \vec{v}^\perp, \quad \vec{S}_\chi, \quad \vec{S}_N$$

with:

$$\left.\begin{aligned} \vec{v}^\perp &= \vec{v} + \frac{\vec{q}}{2\mu_N} \\ \vec{v} &\equiv \vec{v}_{\chi,\mathrm{in}} - \vec{v}_{N,\mathrm{in}} \end{aligned}\right\} \Rightarrow \vec{v}^\perp \cdot \vec{q} = 0$$

$$\begin{aligned}
\mathcal{O}_1 &= 1_\chi 1_N, \\
\mathcal{O}_2 &= (v^\perp)^2, \\
\mathcal{O}_3 &= i\vec{S}_N \cdot \left(\frac{\vec{q}}{m_N} \times \vec{v}^\perp\right), \\
\mathcal{O}_4 &= \vec{S}_\chi \cdot \vec{S}_N, \\
\mathcal{O}_5 &= i\vec{S}_\chi \cdot \left(\frac{\vec{q}}{m_N} \times \vec{v}^\perp\right), \\
\mathcal{O}_6 &= \left(\vec{S}_\chi \cdot \frac{\vec{q}}{m_N}\right)\left(\vec{S}_N \cdot \frac{\vec{q}}{m_N}\right) \\
\mathcal{O}_7 &= \vec{S}_N \cdot \vec{v}^\perp, \\
\mathcal{O}_8 &= \vec{S}_\chi \cdot \vec{v}^\perp, \\
\mathcal{O}_9 &= i\vec{S}_\chi \cdot \left(\vec{S}_N \times \frac{\vec{q}}{m_N}\right), \\
\mathcal{O}_{10} &= i\vec{S}_N \cdot \frac{\vec{q}}{m_N}, \\
\mathcal{O}_{11} &= i\vec{S}_\chi \cdot \frac{\vec{q}}{m_N}.
\end{aligned}$$

A.L.Fitzpatrick, W.Haxton, E.Katz, N.Lubbers and Y.Xu, JCAP1302, 004 (2013),1203.3542;
N.Anand, A.L.Fitzpatrick and W.C.Haxton, Phys.Rev.C89, 065501 (2014),1308.6288.

Additional operators that do not arise for traditional spin≤1 mediators:

$$\mathcal{O}_{12} = \vec{S}_\chi \cdot (\vec{S}_N \times \vec{v}^\perp),$$

$$\mathcal{O}_{13} = i(\vec{S}_\chi \cdot \vec{v}^\perp)\left(\vec{S}_N \cdot \frac{\vec{q}}{m_N}\right),$$

$$\mathcal{O}_{14} = i\left(\vec{S}_\chi \cdot \frac{\vec{q}}{m_N}\right)(\vec{S}_N \cdot \vec{v}^\perp),$$

$$\mathcal{O}_{15} = -\left(\vec{S}_\chi \cdot \frac{\vec{q}}{m_N}\right)\left[(\vec{S}_N \times \vec{v}^\perp) \cdot \frac{\vec{q}}{m_N}\right]$$

$$\mathcal{O}_{16} = -\left[(\vec{S}_\chi \times \vec{v}^\perp) \cdot \frac{\vec{q}}{m_N}\right]\left(\vec{S}_N \cdot \frac{\vec{q}}{m_N}\right)$$

A.L.Fitzpatrick, W.Haxton, E.Katz, N.Lubbers and Y.Xu, JCAP1302, 004 (2013),1203.3542;
N.Anand, A.L.Fitzpatrick and W.C.Haxton, Phys.Rev.C89, 065501 (2014),1308.6288.

Factorization of WIMP physics and nuclear physics

In the expected rate WIMP physics (encoded in the R functions that depend on the c_i couplings) and the nuclear physics (contained in 8 (6+2) response functions W factorize in a simple way:

$$\frac{dR_{\chi T}}{dE_R}(t) = \sum_T N_T \frac{\rho_{\mathrm{WIMP}}}{m_{\mathrm{WIMP}}} \int_{v_{min}} d^3 v_T f(\vec{v}_T, t) v_T \frac{d\sigma_T}{dE_R}$$

$$\frac{d\sigma_T}{dE_R} = \frac{2m_T}{4\pi v_T^2}\left[\frac{1}{2j_\chi+1}\frac{1}{2j_T+1}|\mathcal{M}_T|^2\right]$$

T=target

WIMP

NUCLEUS

$$\frac{1}{2j_\chi+1}\frac{1}{2j_T+1}|\mathcal{M}|^2 = \frac{4\pi}{2j_T+1}\sum_{\tau=0,1}\sum_{\tau'=0,1}\sum_k R_k^{\tau\tau'}\left[c_j^\tau, (v_T^\perp)^2, \frac{q^2}{m_N^2}\right] W_{Tk}^{\tau\tau'}(y)$$

$y \equiv (qb/2)^2$

b=nuclear size

q=momentum transfer

$$k = M,\ \Phi'',\ \Phi''M,\ \tilde{\Phi}',\ \Sigma'',\ \Sigma',\ \Delta, \Delta\Sigma'$$

N.B.: besides usual spin-independent and spin-dependent terms new contributions arise, with explicit dependences on the transferred momentum q and the WIMP incoming velocity

A.L.Fitzpatrick, W.Haxton, E.Katz, N.Lubbers and Y.Xu, JCAP1302, 004 (2013),1203.3542;
N.Anand, A.L.Fitzpatrick and W.C.Haxton, Phys.Rev.C89, 065501 (2014),1308.6288.

WIMPs response funtions

$$R_M^{\tau\tau'}\left(v_T^{\perp 2},\frac{q^2}{m_N^2}\right)=c_1^\tau c_1^{\tau'}+\frac{j_\chi(j_\chi+1)}{3}\left[\frac{q^2}{m_N^2}v_T^{\perp 2}c_5^\tau c_5^{\tau'}+v_T^{\perp 2}c_8^\tau c_8^{\tau'}+\frac{q^2}{m_N^2}c_{11}^\tau c_{11}^{\tau'}\right]$$

$$R_{\Phi''}^{\tau\tau'}\left(v_T^{\perp 2},\frac{q^2}{m_N^2}\right)=\left[\frac{q^2}{4m_N^2}c_3^\tau c_3^{\tau'}+\frac{j_\chi(j_\chi+1)}{12}\left(c_{12}^\tau-\frac{q^2}{m_N^2}c_{15}^\tau\right)\left(c_{12}^{\tau'}-\frac{q^2}{m_N^2}c_{15}^{\tau'}\right)\right]\frac{q^2}{m_N^2}$$

$$R_{\Phi''M}^{\tau\tau'}\left(v_T^{\perp 2},\frac{q^2}{m_N^2}\right)=\left[c_3^\tau c_1^{\tau'}+\frac{j_\chi(j_\chi+1)}{3}\left(c_{12}^\tau-\frac{q^2}{m_N^2}c_{15}^\tau\right)c_{11}^{\tau'}\right]\frac{q^2}{m_N^2}$$

$$R_{\tilde{\Phi}'}^{\tau\tau'}\left(v_T^{\perp 2},\frac{q^2}{m_N^2}\right)=\left[\frac{j_\chi(j_\chi+1)}{12}\left(c_{12}^\tau c_{12}^{\tau'}+\frac{q^2}{m_N^2}c_{13}^\tau c_{13}^{\tau'}\right)\right]\frac{q^2}{m_N^2}$$

$$R_{\Sigma''}^{\tau\tau'}\left(v_T^{\perp 2},\frac{q^2}{m_N^2}\right)=\frac{q^2}{4m_N^2}c_{10}^\tau c_{10}^{\tau'}+\frac{j_\chi(j_\chi+1)}{12}\left[c_4^\tau c_4^{\tau'}+\frac{q^2}{m_N^2}(c_4^\tau c_6^{\tau'}+c_6^\tau c_4^{\tau'})+\frac{q^4}{m_N^4}c_6^\tau c_6^{\tau'}+v_T^{\perp 2}c_{12}^\tau c_{12}^{\tau'}+\frac{q^2}{m_N^2}v_T^{\perp 2}c_{13}^\tau c_{13}^{\tau'}\right]$$

$$R_{\Sigma'}^{\tau\tau'}\left(v_T^{\perp 2},\frac{q^2}{m_N^2}\right)=\frac{1}{8}\left[\frac{q^2}{m_N^2}v_T^{\perp 2}c_3^\tau c_3^{\tau'}+v_T^{\perp 2}c_7^\tau c_7^{\tau'}\right]+\frac{j_\chi(j_\chi+1)}{12}\left[c_4^\tau c_4^{\tau'}+\frac{q^2}{m_N^2}c_9^\tau c_9^{\tau'}+\frac{v_T^{\perp 2}}{2}\left(c_{12}^\tau-\frac{q^2}{m_N^2}c_{15}^\tau\right)\left(c_{12}^{\tau'}-\frac{q^2}{m_N^2}c_{15}^{\tau'}\right)+\frac{q^2}{2m_N^2}v_T^{\perp 2}c_{14}^\tau c_{14}^{\tau'}\right]$$

$$R_{\Delta}^{\tau\tau'}\left(v_T^{\perp 2},\frac{q^2}{m_N^2}\right)=\frac{j_\chi(j_\chi+1)}{3}\left(\frac{q^2}{m_N^2}c_5^\tau c_5^{\tau'}+c_8^\tau c_8^{\tau'}\right)\frac{q^2}{m_N^2}$$

$$R_{\Delta\Sigma'}^{\tau\tau'}\left(v_T^{\perp 2},\frac{q^2}{m_N^2}\right)=\frac{j_\chi(j_\chi+1)}{3}\left(c_5^\tau c_4^{\tau'}-c_8^\tau c_9^{\tau'}\right)\frac{q^2}{m_N^2}.$$

general form:

$$R_k^{\tau\tau'}=R_{0k}^{\tau\tau'}+R_{1k}^{\tau\tau'}\frac{(v_T^\perp)^2}{c^2}=R_{0k}^{\tau\tau'}+R_{1k}^{\tau\tau'}\frac{v_T^2-v_{min}^2}{c^2}$$

Nuclear response functions

Assuming one-body dark matter-nucleon interactions, the Hamiltonian density for dark matter-nucleus interactions is:

$$\begin{aligned}\mathcal{H}_{ET}(\vec{x}) &= \sum_{i=1}^{A} l_0(i)\ \delta(\vec{x}-\vec{x}_i) + \sum_{i=1}^{A} l_0^A(i)\ \frac{1}{2M}\left[-\frac{1}{i}\overleftarrow{\nabla}_i\cdot\vec{\sigma}(i)\delta(\vec{x}-\vec{x}_i)+\delta(\vec{x}-\vec{x}_i)\vec{\sigma}(i)\cdot\frac{1}{i}\overrightarrow{\nabla}_i\right] \\ &+ \sum_{i=1}^{A} \vec{l}_5(i)\cdot\vec{\sigma}(i)\delta(\vec{x}-\vec{x}_i) + \sum_{i=1}^{A} \vec{l}_M(i)\cdot\frac{1}{2M}\left[-\frac{1}{i}\overleftarrow{\nabla}_i\delta(\vec{x}-\vec{x}_i)+\delta(\vec{x}-\vec{x}_i)\frac{1}{i}\overrightarrow{\nabla}_i\right] \\ &+ \sum_{i=1}^{A} \vec{l}_E(i)\cdot\frac{1}{2M}\left[\overleftarrow{\nabla}_i\times\vec{\sigma}(i)\delta(\vec{x}-\vec{x}_i)+\delta(\vec{x}-\vec{x}_i)\vec{\sigma}(i)\times\overrightarrow{\nabla}_i\right]\end{aligned}$$

So the WIMP-nucleus Hamiltonian has the general form:

$$\int d\vec{x}\ e^{-i\vec{q}\cdot\vec{x}}\ \left[l_0\langle J_iM_i|\hat{\rho}(\vec{x})|J_iM_i\rangle - \vec{l}\cdot\langle J_iM_i|\hat{\vec{j}}(\vec{x})|J_iM_i\rangle\right]$$

With:

$$e^{i\vec{q}\cdot\vec{x}_i} = \sum_{J=0}^{\infty}\sqrt{4\pi}\ [J]\ i^J j_J(qx_i)Y_{J0}(\Omega_{x_i})$$

$$\hat{e}_\lambda e^{i\vec{q}\cdot\vec{x}_i} = \begin{cases}\sum_{J=0}^{\infty}\sqrt{4\pi}\ [J]\ i^{J-1}\frac{\vec{\nabla}_i}{q}j_J(qx_i)Y_{J0}(\Omega_{x_i}), & \lambda=0 \\ \sum_{J\geq1}^{\infty}\sqrt{2\pi}\ [J]\ i^{J-2}\left[\lambda j_J(qx_i)\vec{Y}^{\lambda}_{JJ1}(\Omega_{x_i})+\frac{\vec{\nabla}_i}{q}\times j_J(qx_i)\vec{Y}^{\lambda}_{JJ1}(\Omega_{x_i})\right], & \lambda=\pm1\end{cases}$$

A.L.Fitzpatrick, W.Haxton, E.Katz, N.Lubbers and Y.Xu, JCAP1302, 004 (2013),1203.3542;
N.Anand, A.L.Fitzpatrick and W.C.Haxton, Phys.Rev.C89, 065501 (2014),1308.6288.

which depends on the expectations of six distinct nuclear response functions, defined as:

$$
\begin{aligned}
& M_{JM}(q\vec{x}) \\
\Delta_{JM}(q\vec{x}) \quad &\equiv \quad \vec{M}^M_{JJ}(q\vec{x}) \cdot \frac{1}{q}\vec{\nabla} \\
\Sigma'_{JM}(q\vec{x}) \quad &\equiv \quad -i\left\{\frac{1}{q}\vec{\nabla} \times \vec{M}^M_{JJ}(q\vec{x})\right\} \cdot \vec{\sigma} = [J]^{-1}\left\{-\sqrt{J}\ \vec{M}^M_{JJ+1}(q\vec{x}) + \sqrt{J+1}\ \vec{M}^M_{JJ-1}(q\vec{x})\right\} \cdot \vec{\sigma} \\
\Sigma''_{JM}(q\vec{x}) \quad &\equiv \quad \left\{\frac{1}{q}\vec{\nabla} M_{JM}(q\vec{x})\right\} \cdot \vec{\sigma} = [J]^{-1}\left\{\sqrt{J+1}\ \vec{M}^M_{JJ+1}(q\vec{x}) + \sqrt{J}\ \vec{M}^M_{JJ-1}(q\vec{x})\right\} \cdot \vec{\sigma} \\
\tilde{\Phi}'_{JM}(q\vec{x}) \quad &\equiv \quad \left(\frac{1}{q}\vec{\nabla} \times \vec{M}^M_{JJ}(q\vec{x})\right) \cdot \left(\vec{\sigma} \times \frac{1}{q}\vec{\nabla}\right) + \frac{1}{2}\vec{M}^M_{JJ}(q\vec{x}) \cdot \vec{\sigma} \\
\Phi''_{JM}(q\vec{x}) \quad &\equiv \quad i\left(\frac{1}{q}\vec{\nabla} M_{JM}(q\vec{x})\right) \cdot \left(\vec{\sigma} \times \frac{1}{q}\vec{\nabla}\right)
\end{aligned}
$$

with $M_{JM} = j_J Y_{JM}$ Bessel spherical harmonics and $\vec{M}^M_{JL} = j_J \vec{Y}_{JM}$ vector spherical harmonics.

•**M**= vector-charge (scalar, **usual spin-independent part**, non-vanishing for all nuclei)
• **Φ''**=vector-longitudinal, related to spin-orpit coupling σ·l (also spin-independent, non-vanishing for all nuclei)
•**Σ'** and **Σ''** = associated to longitudinal and transverse components of nuclear spin, **their sum is the usual spin-dependent interaction**, require nuclear spin j>0
•**Δ**=associated to the orbital angular momentum operator l, also requires j>0
•**Φ̃'**= related to a vector-longitudinal operator that transforms as a tensor under rotations, requires j>1/2

A.L.Fitzpatrick, W.Haxton, E.Katz, N.Lubbers and Y.Xu, JCAP1302, 004 (2013),1203.3542;
N.Anand, A.L.Fitzpatrick and W.C.Haxton, Phys.Rev.C89, 065501 (2014),1308.6288.

Coupling – nuclear response function correspondence

coupling	$R_{0k}^{\tau\tau'}$	$R_{1k}^{\tau\tau'}$	coupling	$R_{0k}^{\tau\tau'}$	$R_{1k}^{\tau\tau'}$
1	$M(q^0)$	-	3	$\Phi''(q^4)$	$\Sigma'(q^2)$
4	$\Sigma''(q^0)$,$\Sigma'(q^0)$	-	5	$\Delta(q^4)$	$M(q^2)$
6	$\Sigma''(q^4)$	-	7	-	$\Sigma'(q^0)$
8	$\Delta(q^2)$	$M(q^0)$	9	$\Sigma'(q^2)$	-
10	$\Sigma''(q^2)$	-	11	$M(q^2)$	-
12	$\Phi''(q^2)$,$\tilde{\Phi}'(q^2)$	$\Sigma''(q^0)$,$\Sigma'(q^0)$	13	$\tilde{\Phi}'(q^4)$	$\Sigma''(q^2)$
14	-	$\Sigma'(q^2)$	15	$\Phi''(q^6)$	$\Sigma'(q^4)$

$$R_k^{\tau\tau'} = R_{0k}^{\tau\tau'} + R_{1k}^{\tau\tau'} \frac{(v_T^\perp)^2}{c^2} = R_{0k}^{\tau\tau'} + R_{1k}^{\tau\tau'} \frac{v_T^2 - v_{min}^2}{c^2}$$

Nuclear response functions at zero momentum transfer

$$\frac{16\pi}{(j_T+1)} \times W^{p}_{Tk}(y=0) \qquad\qquad \frac{16\pi}{(j_T+1)} \times W^{n}_{Tk}(y=0)$$

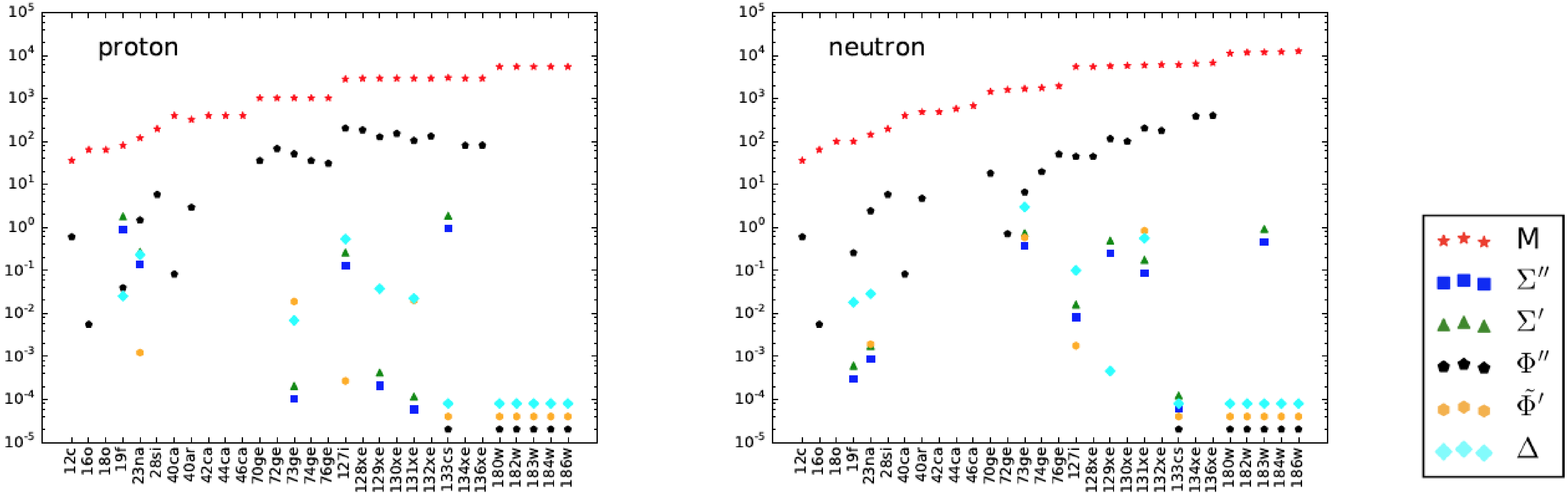

Normalization of W's chosen so that:

$$\frac{16\pi}{(j_T+1)} \times W^{p}_{TM}(y=0) = Z_T \qquad\qquad \frac{16\pi}{(j_T+1)} \times W^{n}_{TM}(y=0) = A_T - Z_T$$

N.B. different scalings of the WIMP-nucleus cross section with the target nuclei

Factorization of astrophysics

The expected rate in a direct detection experiment can be written as:

$$R = \int_0^\infty \mathcal{R}(v)\tilde{\eta}(v)\,dv = \int_0^\infty \mathcal{R}'(E_R)\tilde{\eta}'(E_R)\,dE_R$$

where R is a response function that depends on the experimental inputs and on the scaling law, while η is a halo function that depends on astrophysics (WIMP local denity and velocity distribution:

$$\tilde{\eta}(v) = \frac{\rho_\chi}{m_\chi}\sigma\eta(v), \quad \eta(v) = \int_v^{v_{esc}} \frac{f(v)}{v}\,dv,$$

For N large enough can approximate:

$$\tilde{\eta}(v) = \sum_{k=1}^{N} \delta\tilde{\eta}^k \theta(v_k - v)$$

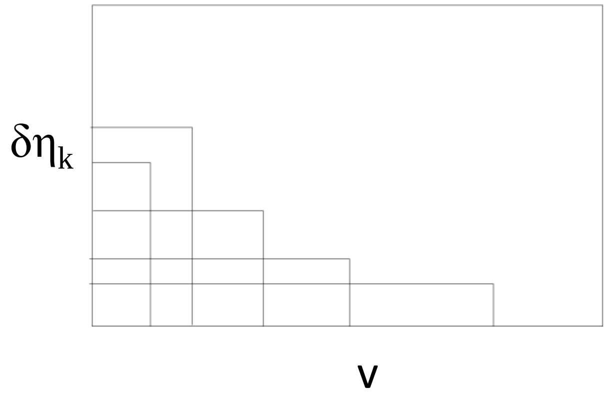

and including explicit velocity dependence:

$$\mathcal{R}(v) = \mathcal{R}_0 + \mathcal{R}_1(v^2 - v_{min}^2)$$

with:

$$v_{min} = \frac{1}{2m_N E_R}\left|\frac{m_N E_R}{\mu_{\chi N}} + \delta\right|$$

The rate can be written as

$$R = \sum_{k=1}^{N} \delta\tilde{\eta}^k \times$$

$$\Big\{\bar{\mathcal{R}}_0\left[E_R^{max}(v_k)\right] + (v_k^2 - \frac{\delta}{\mu_{\chi N}})\bar{\mathcal{R}}_1\left[E_R^{max}(v_k)\right]$$

$$-\frac{m_N}{2\mu_{\chi N}^2}\bar{\mathcal{R}}_{1E}\left[E_R^{max}(v_k)\right] - \frac{\delta^2}{2m_N}\bar{\mathcal{R}}_{1E^{-1}}\left[E_R^{max}(v_k)\right]\Big\}$$

In terms of four response functions that do not depend on the WIMP mass or mass splitting:

$$\bar{\mathcal{R}}_{0,1}(E_R) \equiv \int_0^{E_R} dE'_R \mathcal{R}_{0,1}(E'_R)$$

$$\bar{\mathcal{R}}_{1E}(E_R) \equiv \int_0^{E_R} dE'_R E'_R \mathcal{R}_1(E'_R)$$

$$\bar{\mathcal{R}}_{1E^{-1}}(E_R) \equiv \int_0^{E_R} dE'_R \frac{1}{E'_R} \mathcal{R}_1(E'_R)$$

that can be tabulated for later use.

- We assume that one coupling dominates at a time (14 cases)
- We calculate exclusion plots from 15 existing experiments: XENON1T, PANDAX-II, KIMS, CDMSlite, SuperCDMS, COUPP, PICASSO, PICO-60 (using a CF_3I target and a C_3F_8 one) CRESST-II, DAMA modulation data), DAMA0 (average count rate), CDEX, DAMIC and DarkSide-50
- We include projections from LZ, COSINUS, PICO500 (a CF_3I target and a C_3F_8)

Sensitivity reach expressed in terms of 90% C.L. bounds on effective cross section:

$$\sigma_{\mathcal{N}} = \max(\sigma_p, \sigma_n)$$

$$\sigma_p = (c_j^p)^2 \frac{\mu_{\chi\mathcal{N}}^2}{\pi} \qquad \sigma_n = (c_j^n)^2 \frac{\mu_{\chi\mathcal{N}}^2}{\pi}$$

N.B. Corresponds to long-distance point-like cross section for standard SI and SD interactions. In other cases just a convenient alternative to directly parameterizing the interaction in terms of the c_j^p coupling.

Tabulate full calculation of R response function for each:

1) Experiment
2) Energy bin/energy threshold/energy value
3) Isospin value (c_n/c_p=-1,0,1)
4) Nuclear target (including all stable isotopes)
5) Effective coupling
6) 4 terms including explicit velocity dependence

Isospin rotation with $r=c^n/c^p$:

$$R(r) = \frac{r(r+1)}{2} R(r=1) + (1-r^2) R(r=0) + \frac{r(r-1)}{2} R(r=-1)$$

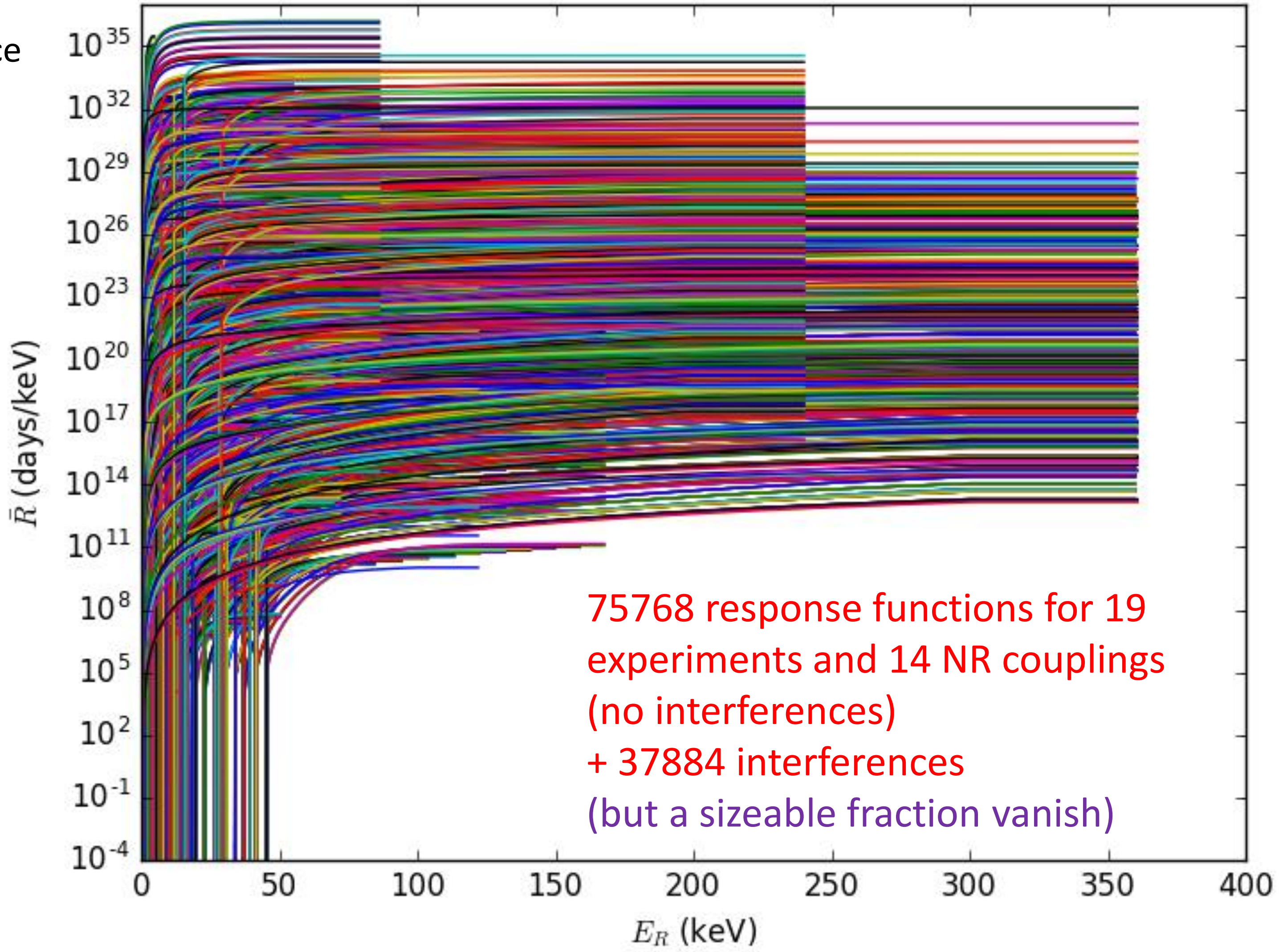

Schematic behaviors of the $\bar{R}_0$ functions

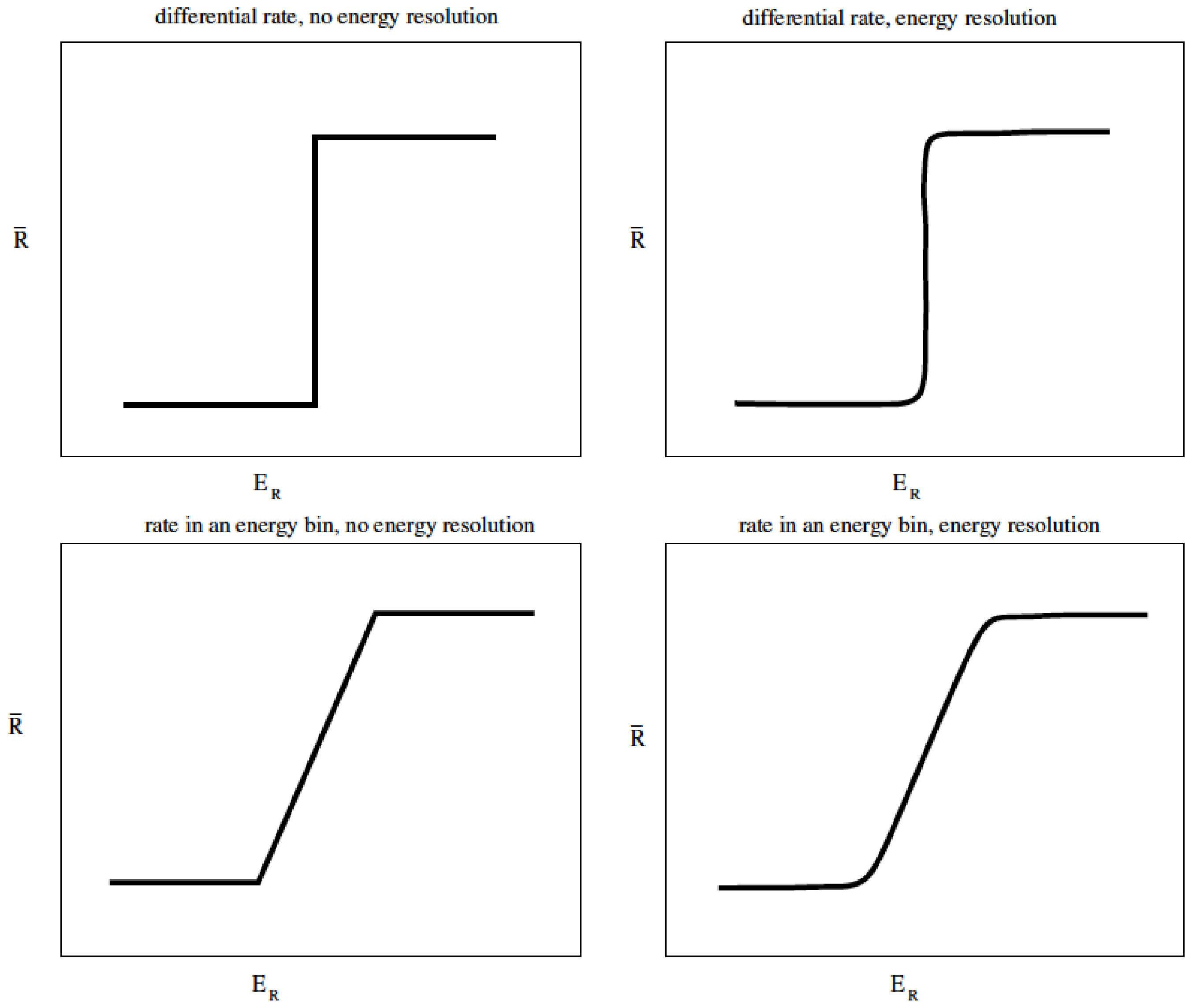

Sunghyun Kang, S.S., G. Tomar, J.H. Yoon, arXiv:1805.06113

- Two free parameters: WIMP mass m_χ and $r=c^n/c^p$
- A different exclusion plot for each c^n/c^p
- We show contour plots in the m_χ and c^n/c^p plane of $\sigma_{N,lim}$ - also indicate with a different color code the most constraining experiment

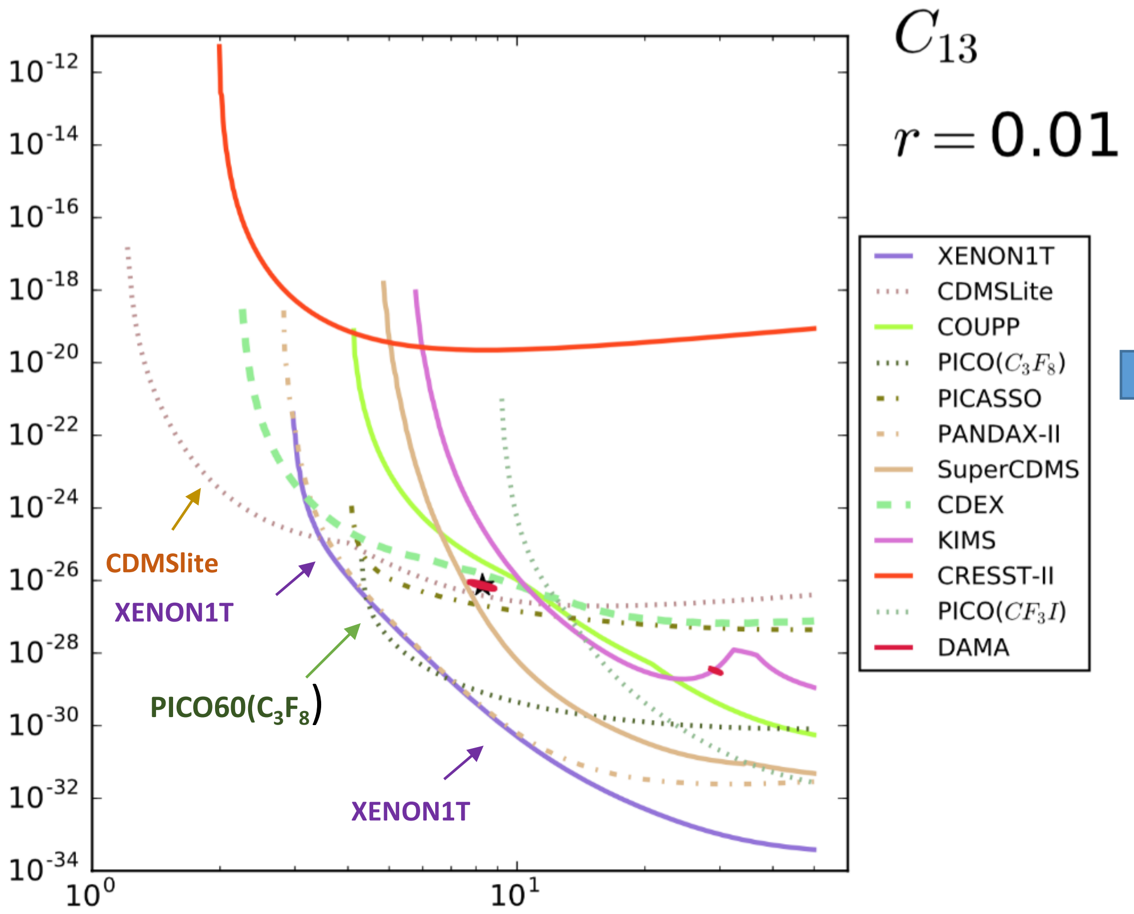

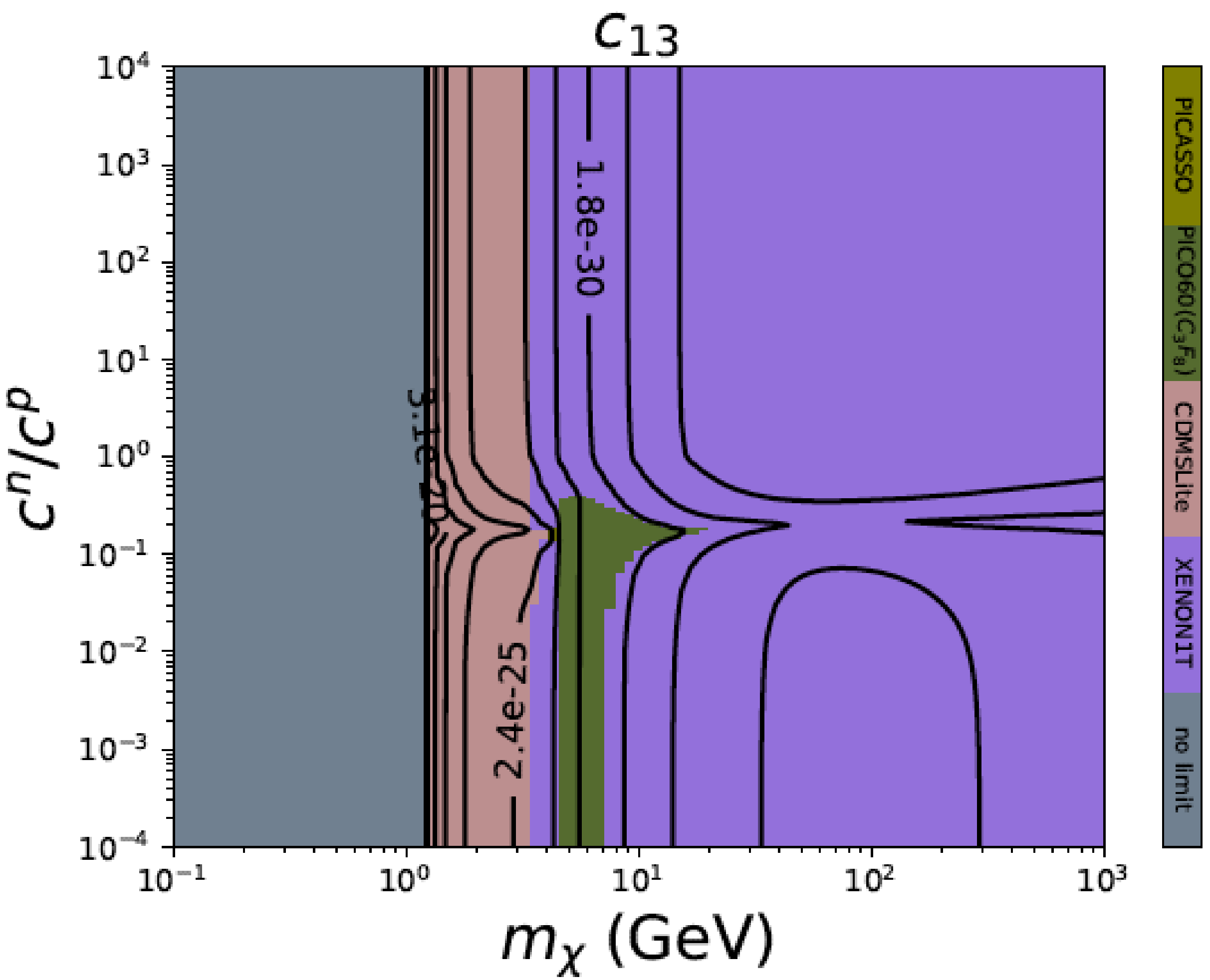

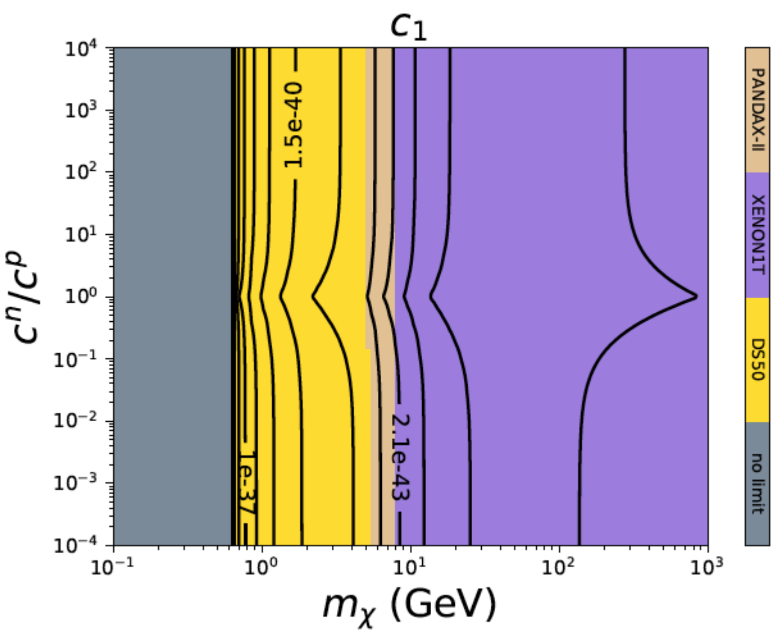

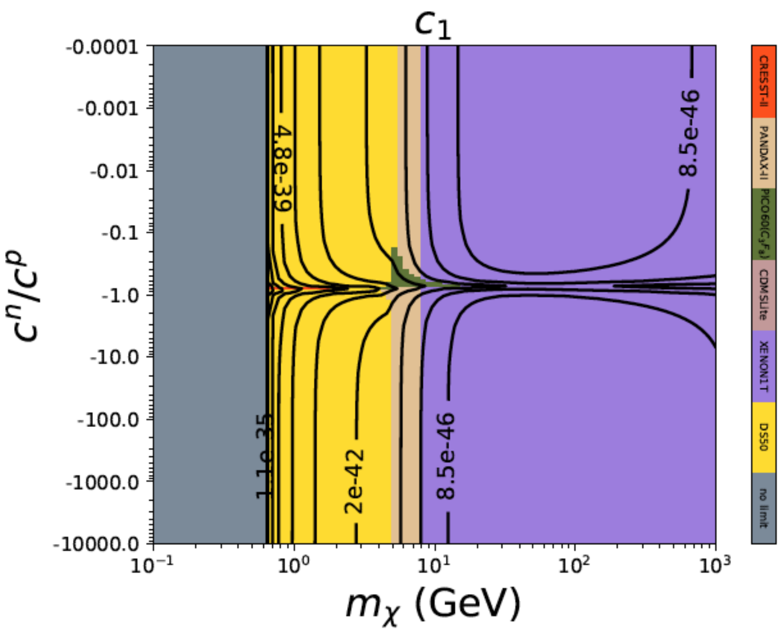

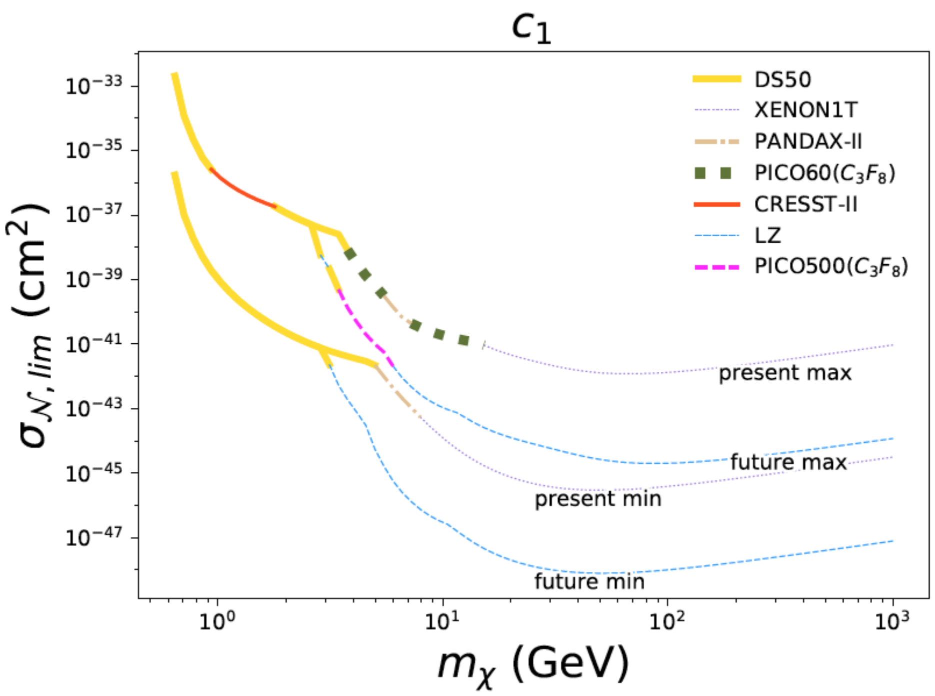

Standard spin-independent coupling

M nuclear response

No velocity dependence in the cross section

Favors heavy nuclei with the exception of low WIMP masses

Similar behavior: c_{11} (q^2)

Sunghyun Kang, S.S., G. Tomar, J.H. Yoon, arXiv:1805.06113

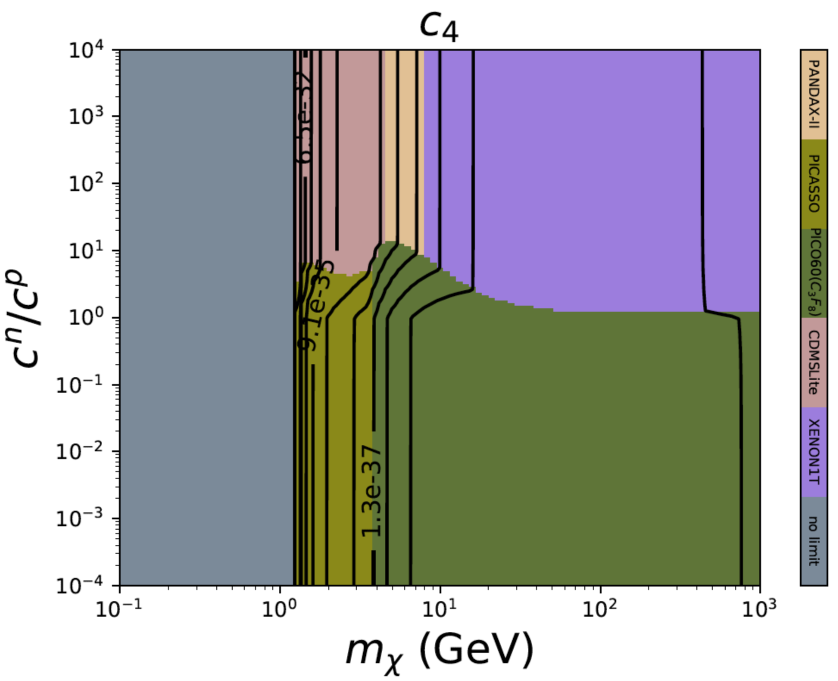

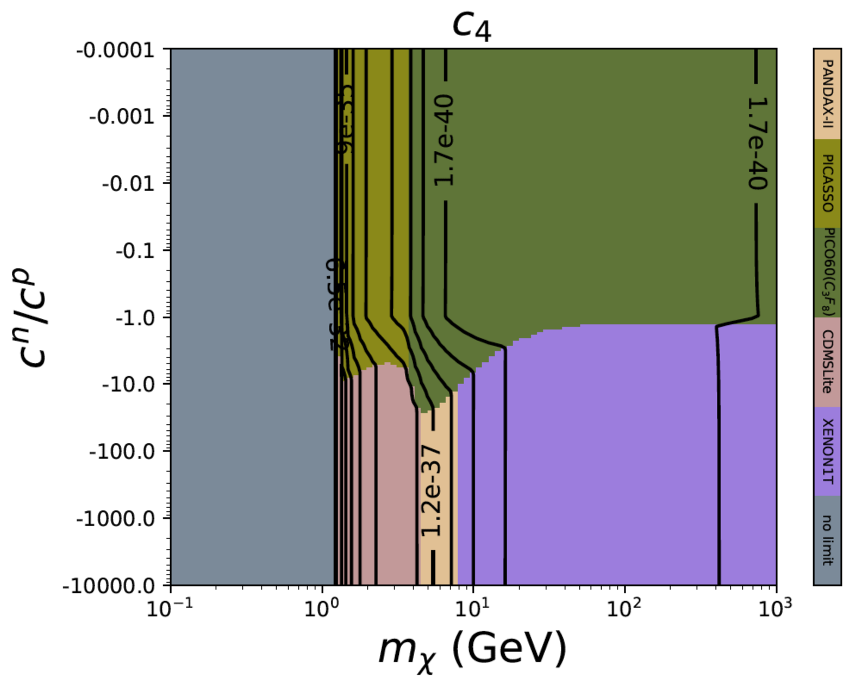

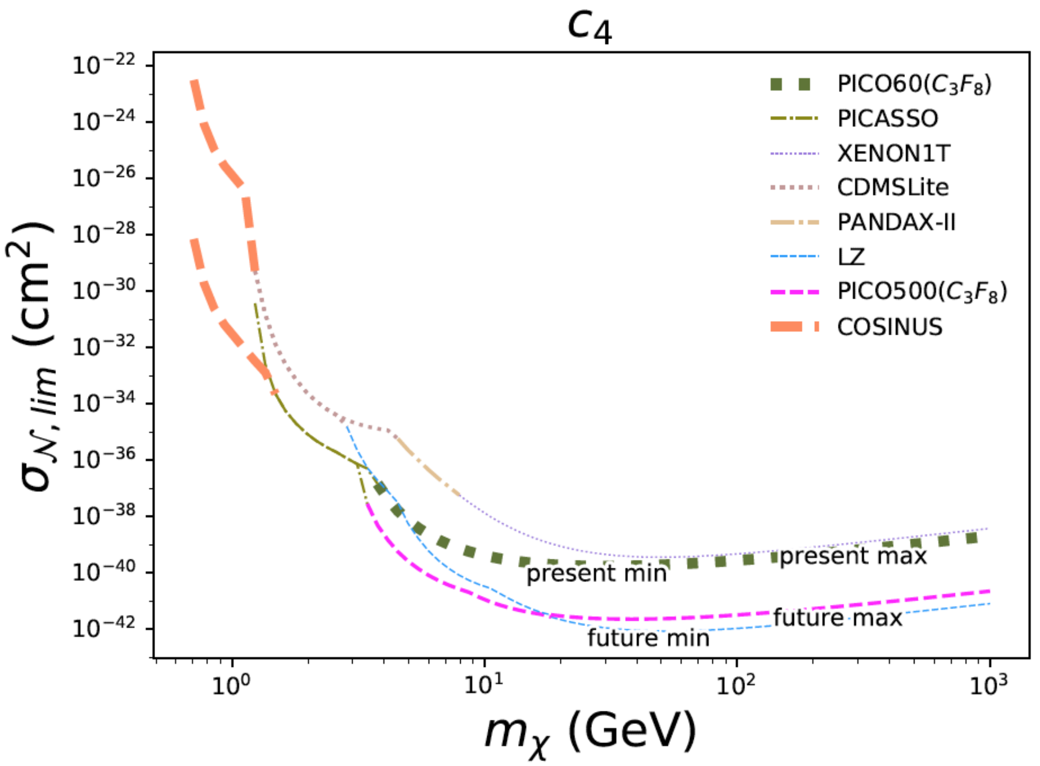

Standard spin-dependent coupling

Σ', Σ'' response functions

No velocity dependence in the cross section

Favors proton-odd targets (fluorine,iodine) for $c^n/c^p><$

and neutron-odd targets (xenon, germanium) for $c^n/c^p>1$

Similar behavior: c_9, c_{10} (q^2) and c_{10} (q^4)

Sunghyun Kang, S.S., G. Tomar, J.H. Yoon, arXiv:1805.06113

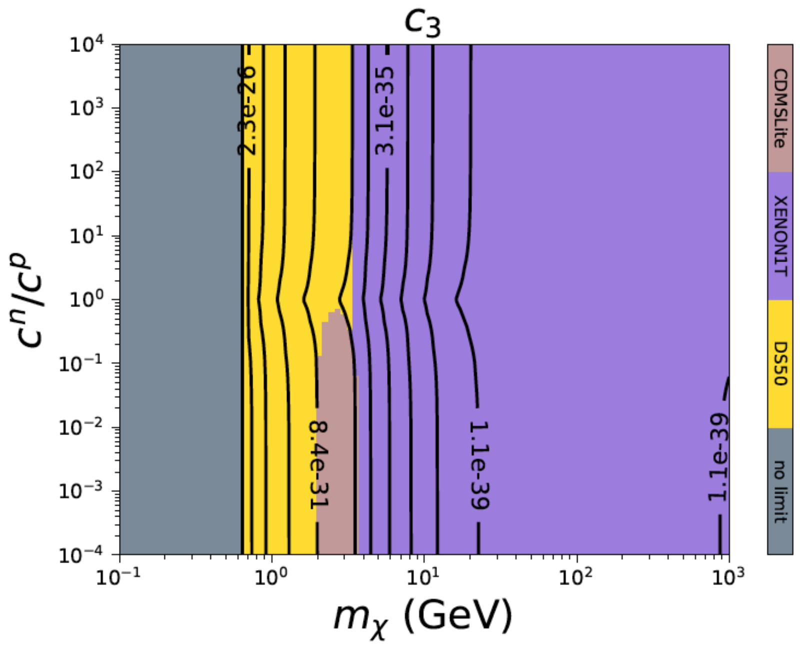

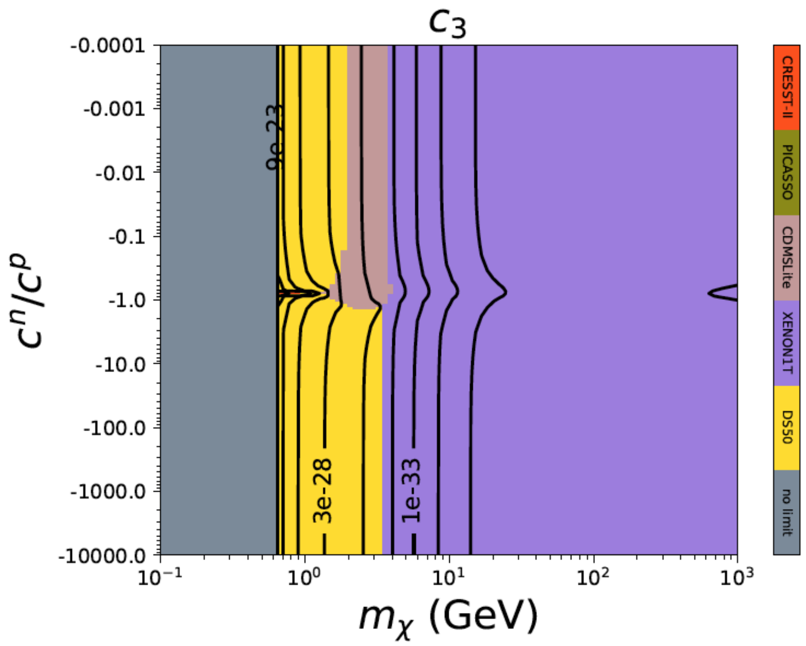

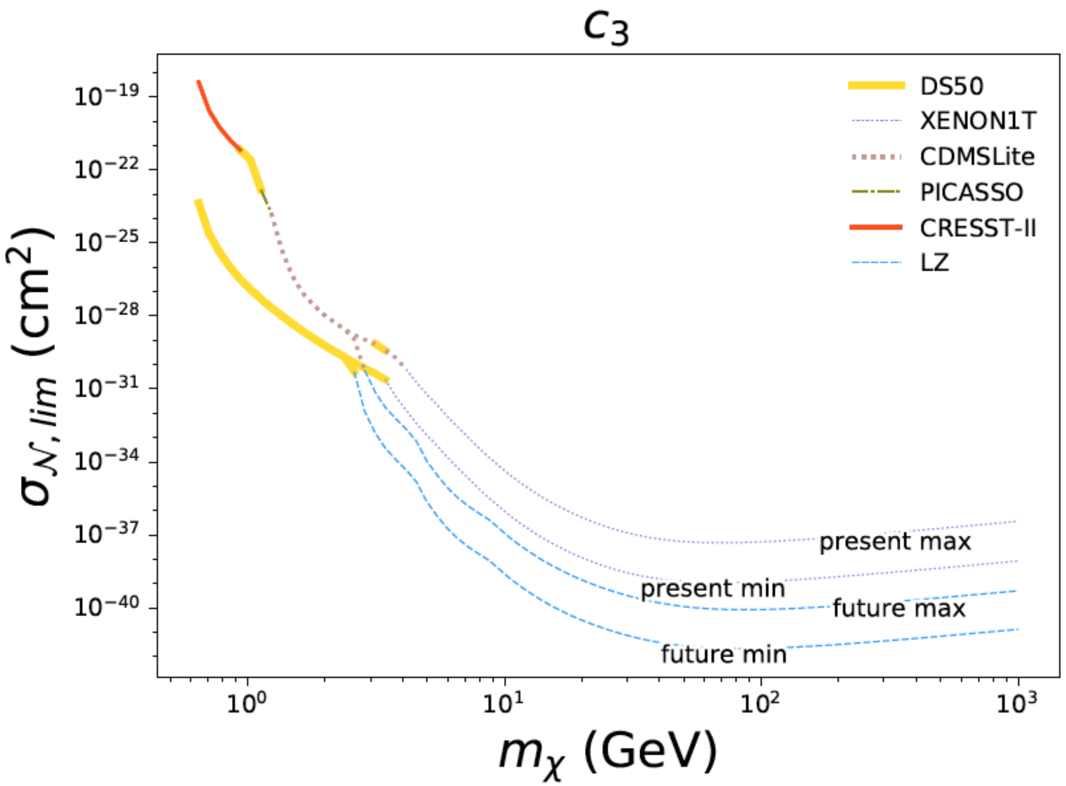

Φ'' response function (related to spin-orbit coupling, non vanishing for all nuclei)

Favors heavier elements (with the exception of low WIMP masses) with large nuclear shell model orbitals not fully occupied

Vanishes for semi-magic isotopes (e.g. ^{72}Ge, explains weakening of CDMSlite bound for $c^n/c^p>1$)

Similar behavior: c_{12} (q^2), c_{15} (q^6)

Sunghyun Kang, S.S., G. Tomar, J.H. Yoon, arXiv:1805.06113

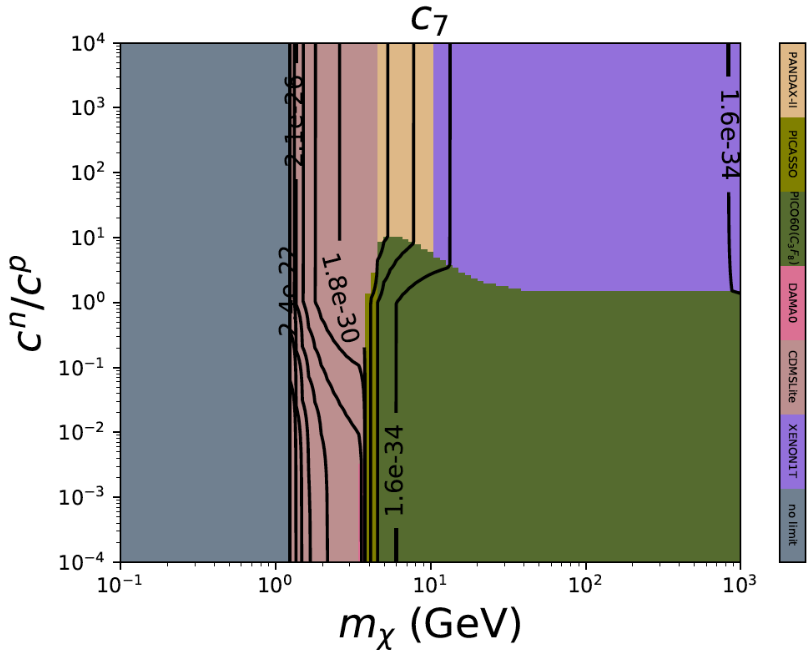

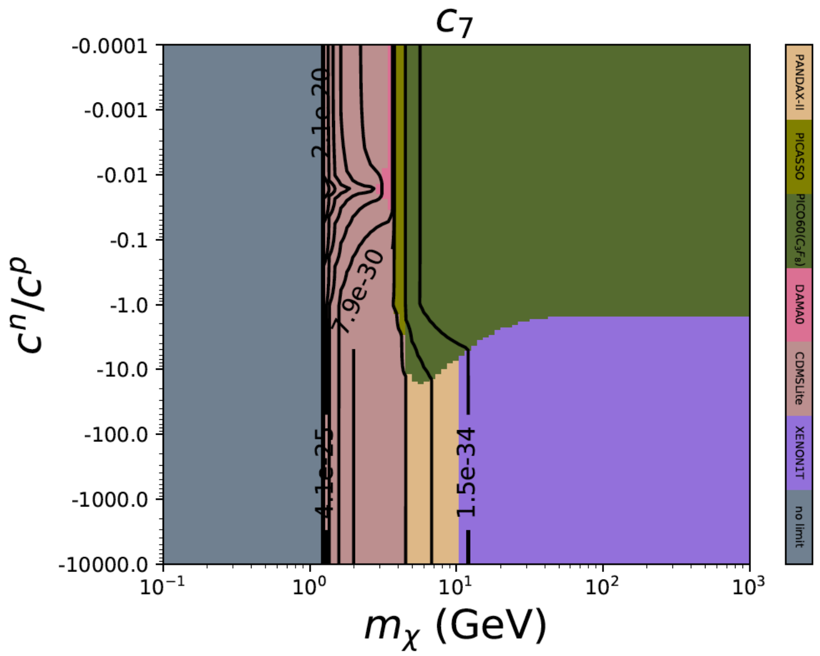

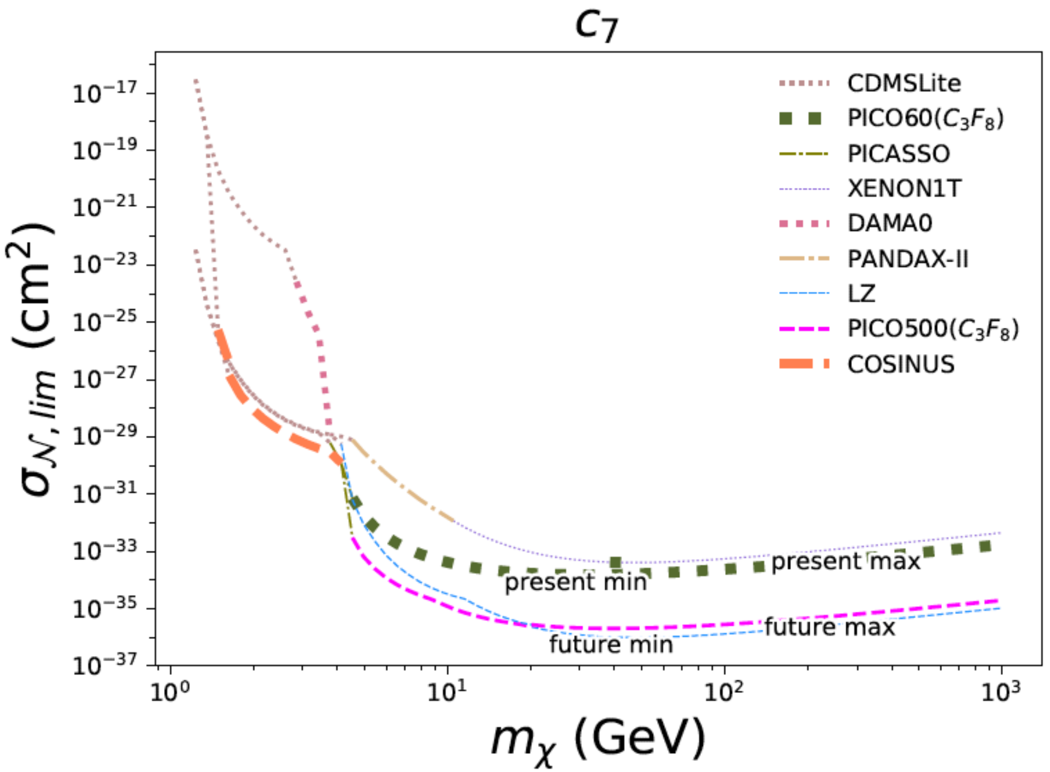

Σ’ response function

Favors proton-odd targets (fluorine,iodine) for c^n/c^p><

and neutron-odd targets (xenon, germanium) for c^n/c^p>1

Only velocity dependent term in the cross section

(cfr. standard SD: low threshold less important, rate dominated by $v \gg v_{min}$, explains reduced PICASSO sensitivity at low WIMP mass compared to c_4)

Similar behavior: c_{14} (q^2)

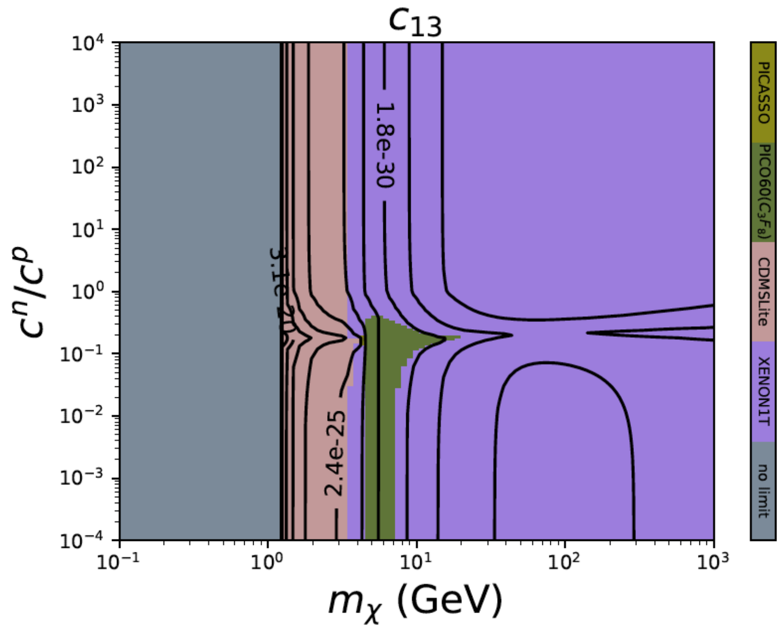

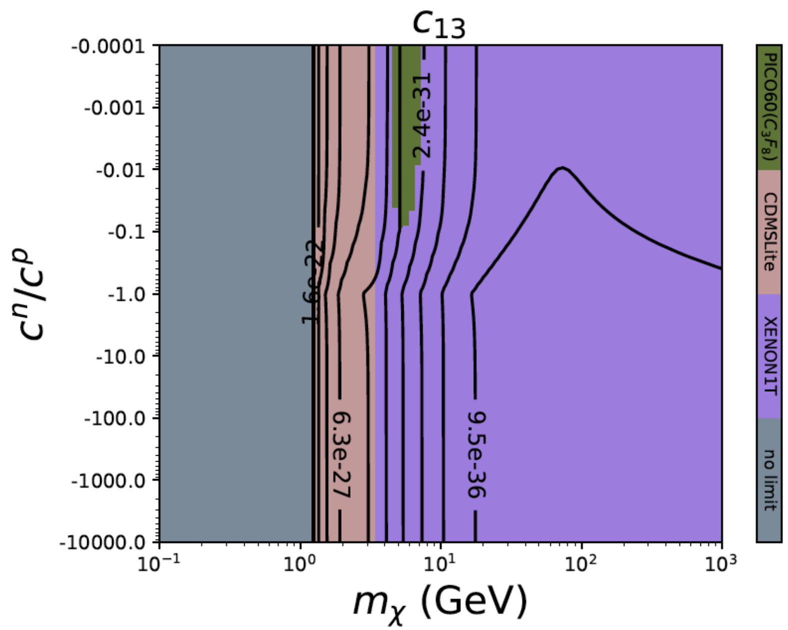

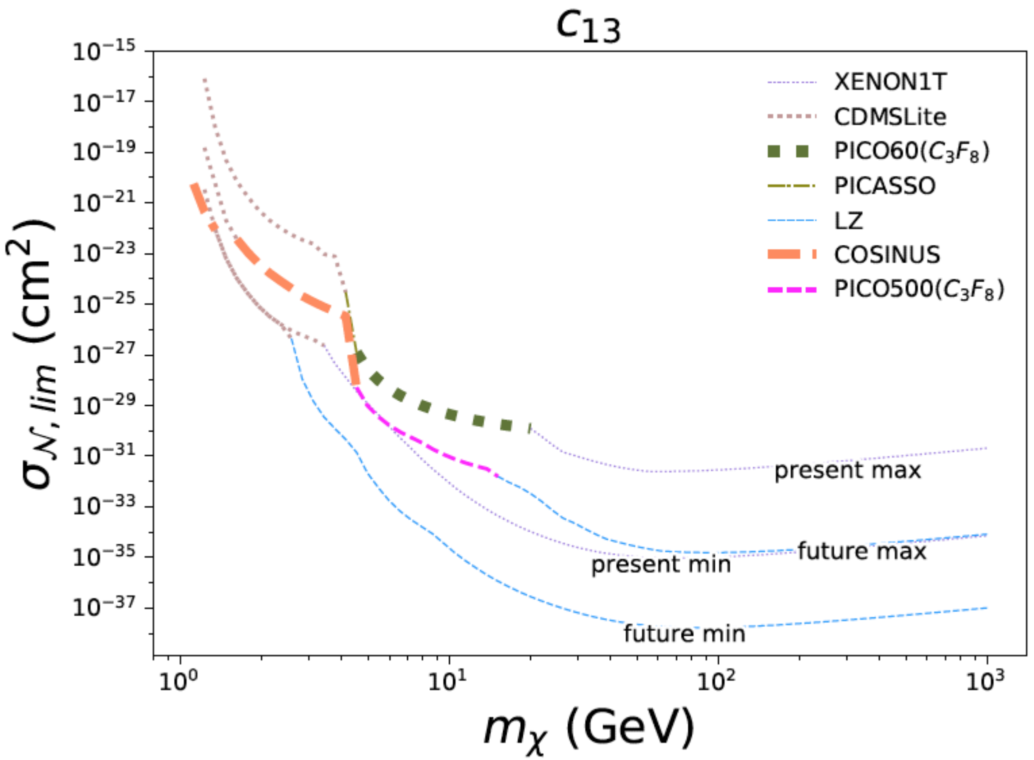

$\tilde{\Phi}''$ response function in velocity-independent part (related to vector-longitudinal operator that transforms as a tensor under rotations, requires nuclear spin >1/2, non-vanishing only for ^{23}Na, ^{73}Ge, ^{121}I and ^{131}Xe among available targets)

Velocity dependent terms off fluorine competitive to velocity-independent term in xenon, explains PICO60(C_3F_8) competitiveness.

Sunghyun Kang, S.S., G. Tomar, J.H. Yoon, arXiv:1805.06113

Coupling	Present		Future	
	m_χ (GeV)	$\sigma_{\mathcal{N},lim}(\mathrm{cm}^2)$	m_χ (GeV)	$\sigma_{\mathcal{N},lim}(\mathrm{cm}^2)$
c_1	50.9	2.9×10^{-46}	50.9	7.9×10^{-49}
c_3	67.3	1.1×10^{-39}	81.1	2.1×10^{-42}
c_4	29.1	1.7×10^{-40}	50.8	8.5×10^{-43}
c_5	61.4	2.9×10^{-37}	67.3	7.0×10^{-40}
c_6	73.9	2.1×10^{-35}	89.0	3.3×10^{-38}
c_7	32.0	1.5×10^{-34}	46.4	9.9×10^{-37}
c_8	50.9	1.2×10^{-39}	55.9	3.3×10^{-42}
c_9	55.9	1.9×10^{-37}	55.9	4.9×10^{-40}
c_{10}	61.4	3.3×10^{-38}	81.1	6.9×10^{-41}
c_{11}	61.4	2.8×10^{-43}	67.3	7.1×10^{-46}
c_{12}	61.3	2.6×10^{-41}	67.3	6.1×10^{-44}
c_{13}	67.3	9.5×10^{-36}	89.0	1.7×10^{-38}
c_{14}	55.9	4.2×10^{-31}	61.4	1.1×10^{-33}
c_{15}	73.9	6.3×10^{-37}	89.0	9.1×10^{-40}

Sunghyun Kang, S.S., G. Tomar, J.H. Yoon, arXiv:1805.06113

Inelastic Dark Matter

D. Tucker-Smith and N.Weiner, Phys.Rev.D 64, 043502 (2001), hep-ph/0101138

Two mass eigenstates χ and χ' very close in mass: $m_{\chi}-m_{\chi'}\equiv\delta$ with χ +N→ χ +N forbidden

"Endothermic "scattering ($\delta>0$)

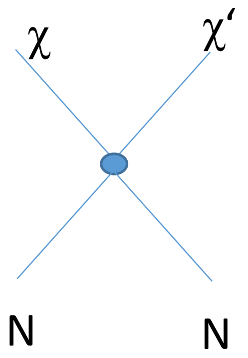

Kinetic energy needed to "overcome" step → rate no longer exponentially decaying with energy, maximum at finite energy E_*

"Exothermic" scattering ($\delta<0$)

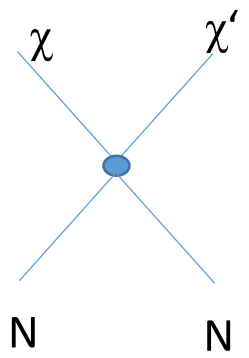

χ is metastable, δ energy deposited independently on initial kinetic energy (even for WIMPs at rest)

Can easily generalize the analysis **to inelastic scattering** (the response functions do not change, only the mapping between recoil energy and WIMP speed)

For inelastic DM the recoil energy E_R is no longer monotonically growing with v_{min} , WIMPs need at least the speed $\min(v_{min})=v_*$ to produce upscattering to heavy state

$$v_{min} = \frac{1}{\sqrt{2m_N E_R}}\left(\frac{m_N E_R}{\mu}+\delta\right) = a\sqrt{E_r}+\frac{b}{\sqrt{E_R}}$$

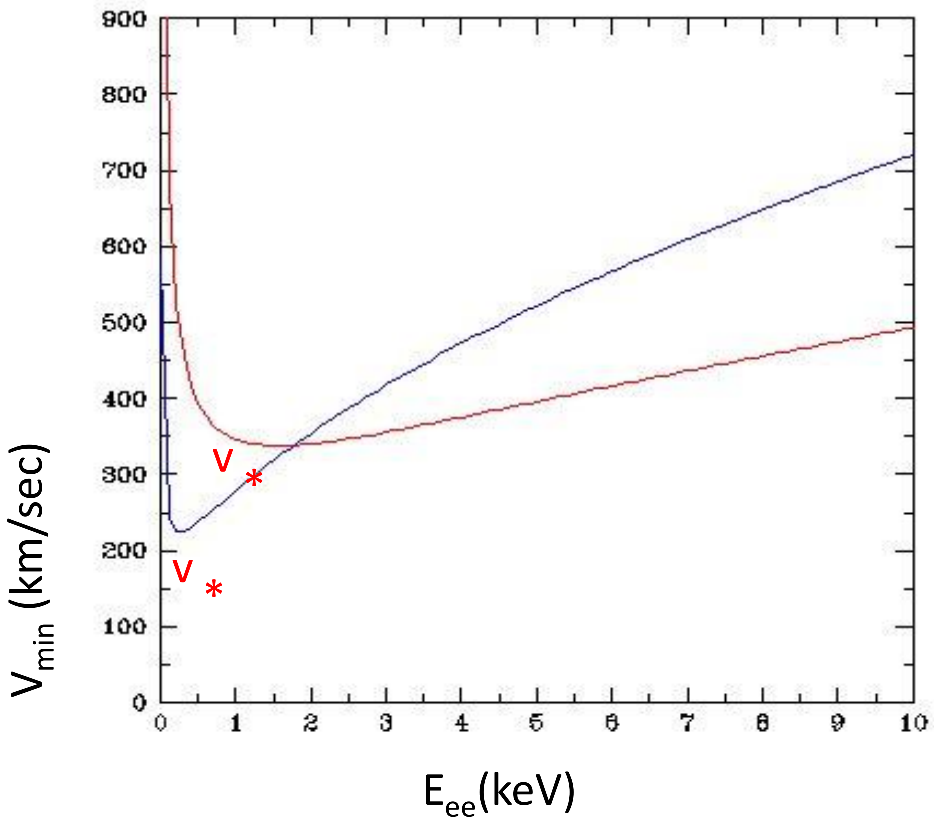

N.B. for δ>0 WIMPs need a minimal absolute incoming speed v_* to upscatter to the heavier state → vanishing rate if $v_* > v_{esc}$ (escape velocity)

Inelastic scattering favors heavy elements, for each isotope inelastic upscatters become kinematically forbidden beyond maximal mass splitting δ corresponsing to escape velocity in the Galaxy

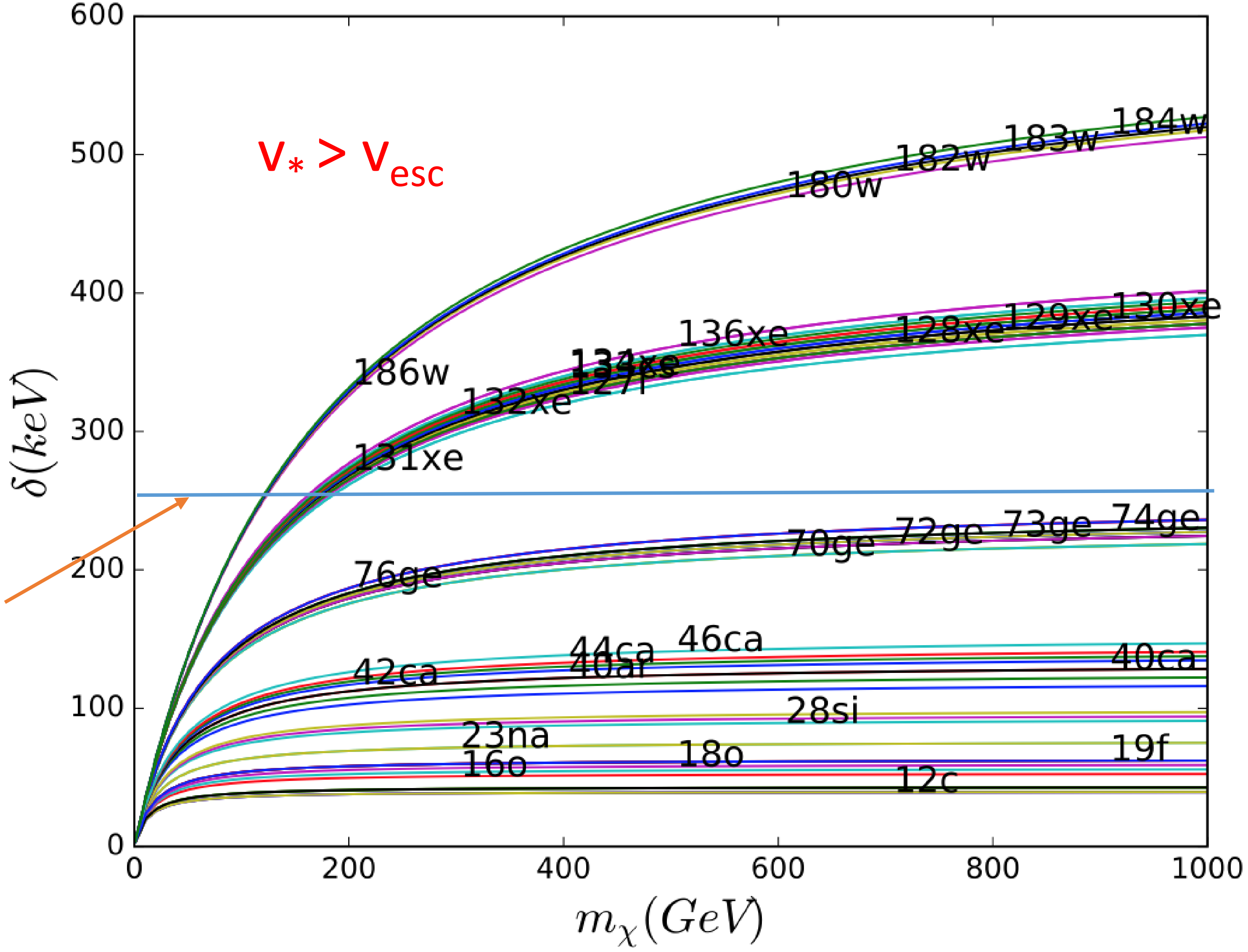

For instance, for δ>250 keV only Xenon, Iodine and Tungsten can detect IDM

Can easily generalize the analysis **to inelastic scattering** (the response functions do not change, only the mapping between recoil energy and WIMP speed)

$\delta=0$

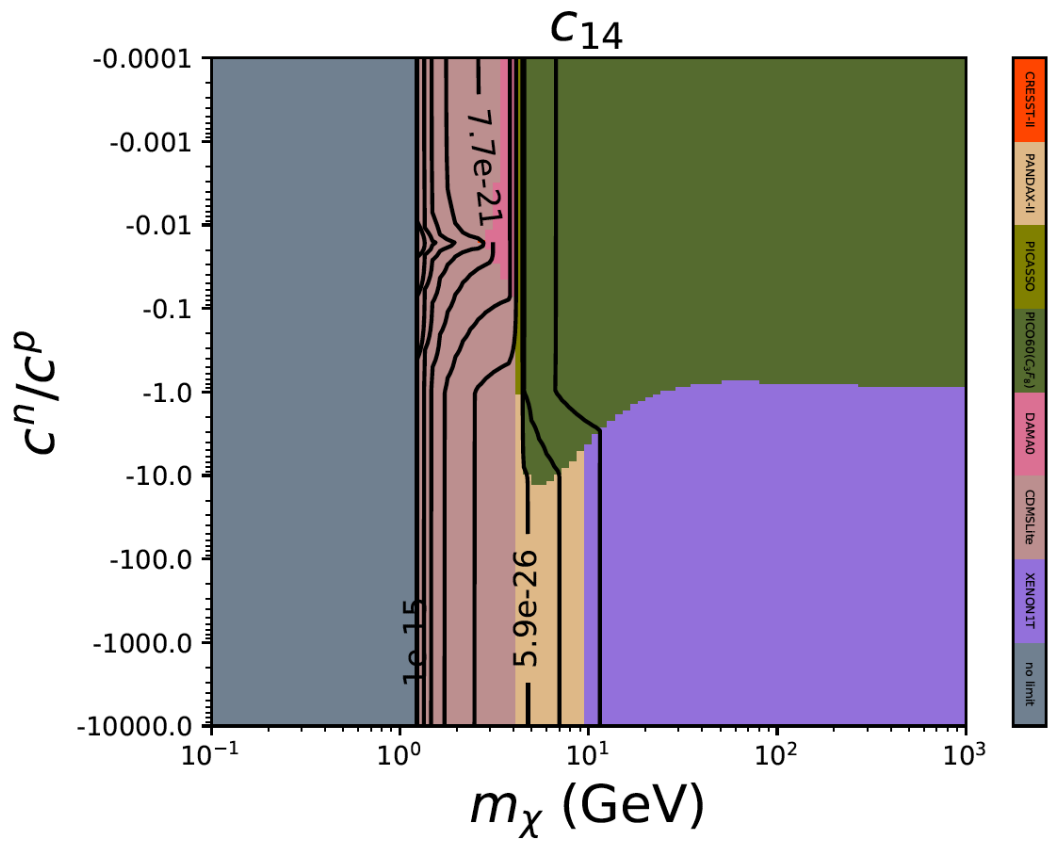

$\delta=50$ keV

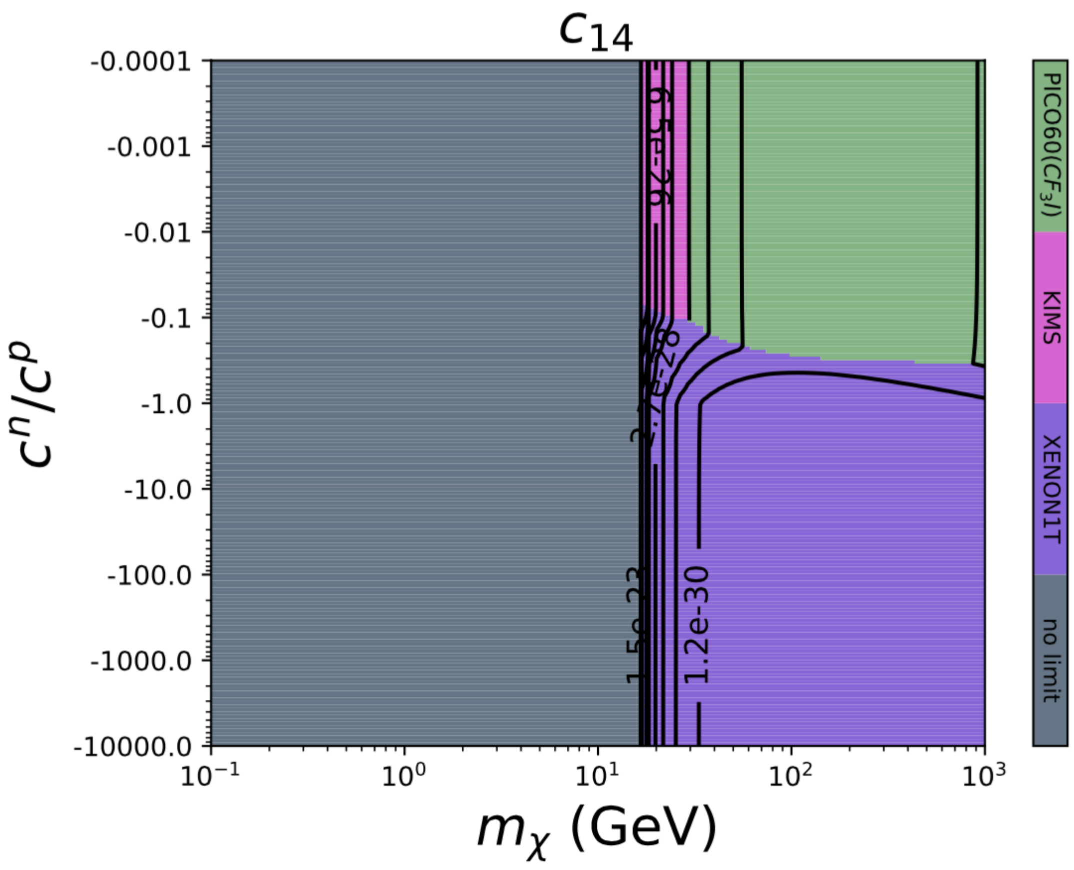

fluorine→iodine for $c^n/c^p>1$

Sunghyun Kang, S.S., G. Tomar, J.H. Yoon, work in progress

- expected reach on $\sigma_{N,lim}$ varies by many orders of magnitude with the effective coupling.
- In most cases it is either driven by a
  - **xenon target**, as for c_1, c_3, c_5, c_8, c_{11}, c_{12}, $c1_3$ and c_{15} (XENON1T among existing experiments and LZ among future ones)
  - **fluorine target** as for c_4, and c_7, (PICO-60 ($C_3 F_8$) among existing experiments and PICO-500 ($C_3 F_8$) among future ones).
- 9 present experiments out of the total of 15 considered provide the most stringent bound on some of the effective couplings for a given choice of m_χ, c^n / c^p) : XENON1T, PANDAX-II, CDMSlite, PICASSO,PICO-60 ($C_3 F_8$) ($CF_3 I$), PICO-60 ($C_3 F_8$) , CRESST-II, DAMA0 (average count rate) and DarkSide-50 → complementarity of
- different target nuclei and/or different combinations of count-rates and energy thresholds when the search of a DM particle is extended to a wide range of possible interactions.
- The variation of the best reach on $\sigma_{N,lim}$ with , c^n / c^p is about:
  - 3 orders of magnitude for c_1 , c_{11} and c_{13}
  - 1 order of magnitude for c_{13}, c_5, c_8 , c_{12}, c_{15}
  - order one for c_4, c_6, c_7 , c_9, c_{10}, c_{14}
- For all couplings future experiments could improve the present best reach between two and three orders of magnitude.
- For inelastic DM WIMP-proton scatterings can be kinematically not accessible to Fluorine → Iodine becomes important in this case

- harder energy spectrum of the expected signal compared to the usual exponentially decaying case for non-standard interactions with a cross section which depends explicitly on the momentum transfer q. We included this effect when i) subtracting the background ii) applying the Optimal Interval method.
- Typically background subtraction plays a role in experiments with a low threshold that target light WIMPs. In this case the spectrum depends on the high-speed tail of the velocity distribution and momentum dependence has a limited effect on the spectral shape → limited effect on the exclusion plot.

DAMA phase2 in effective models

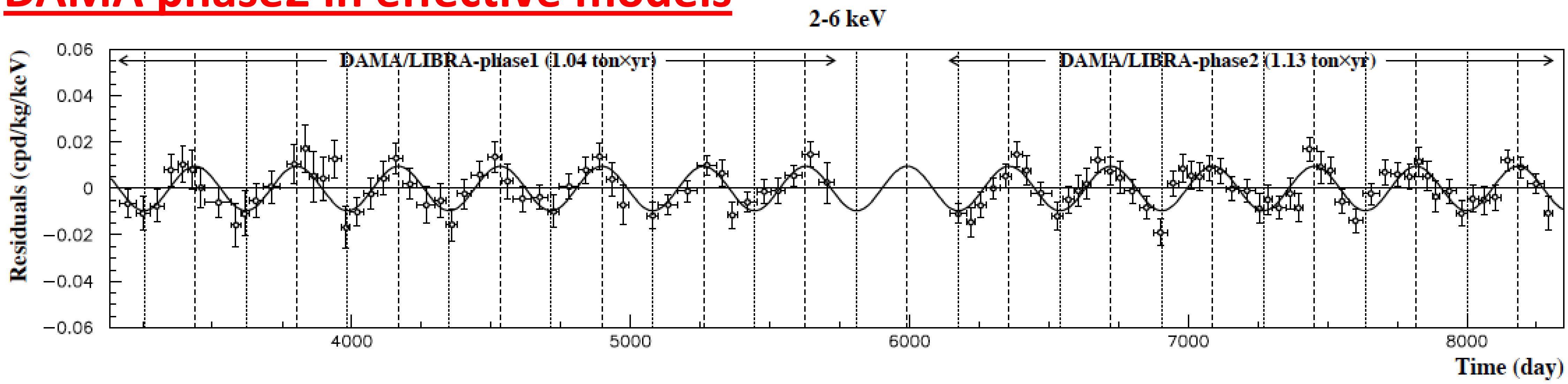

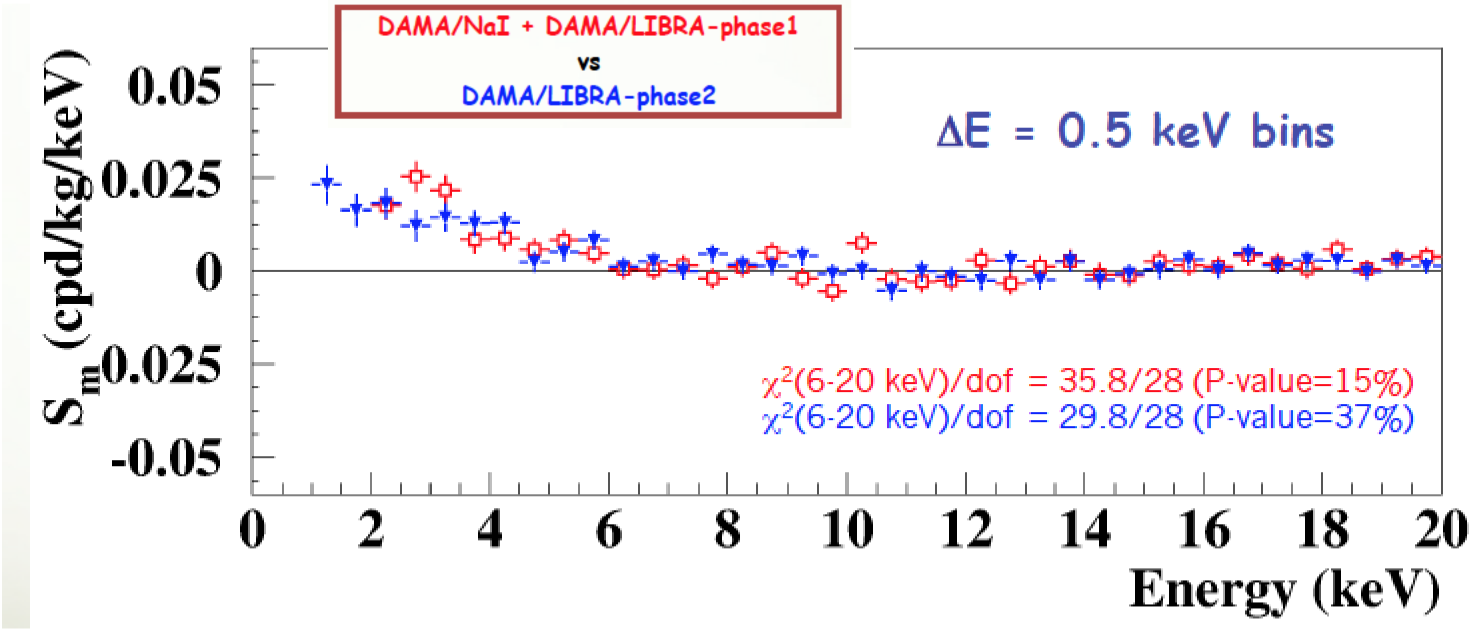

$$R(t) = S_0 + S_m \cos[\omega(t - t_0)]$$

$$\omega = 2\pi/(1 \text{ year})$$

$$t_0 = 152.5\text{day}$$

Bernabei et al. (DAMA Collaboration), 1805.10486

- no fit of the DAMA result is available in the literature in terms of non–relativistic EFT models
- in addition to increasing the exposure, the phase2 result also includes a lower energy threshold, and the new spectrum of modulation amplitudes no longer shows a maximum, but is rather monotonically decreasing with energy
- We extended an assessment of the goodness of fit of the new DAMA result to NREFT scenarios
- Assume a standard Maxwellian for the WIMP velocity distribution in the Galaxy

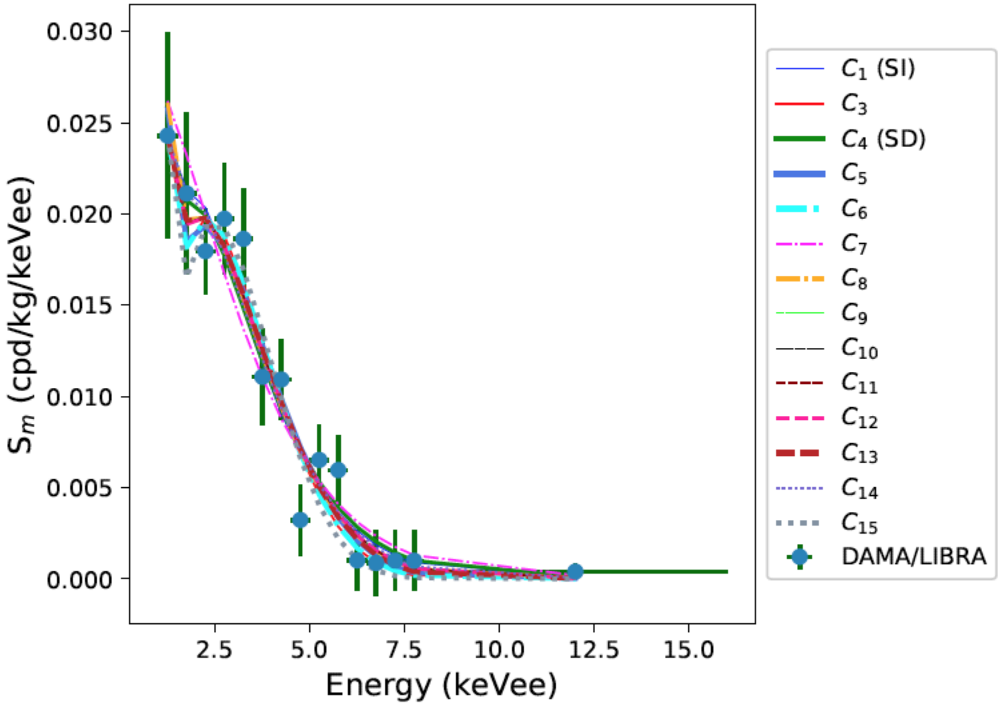

3-parameter fit (WIMP mass m_χ, WIMP-proton cross section σ_p, $r=c^n/c^p$) assuming that one of the EFT couplings dominates

Sunghyun Kang, S.S., G. Tomar, J.H. Yoon, arXiv:1804.07528

- With a lower threshold now DAMA is sensitive to WIMP-Iodine scatterings also at low mass
- In the SI case Iodine contribution is large and steeply decaying with energy → need to tune c^n/c^p to suppress Iodine contribution (S. Baum,K. Freese and C. Kelso, 1804.01231)
- if the WIMP–nucleus cross section is driven by other operators the fine tuning required to suppress iodine is reduced and/or the hierarchy between the WIMP–iodine and the WIMP–sodium cross section is less pronounced in the first place
- effective models for which the cross section depends explicitly on the WIMP incoming velocity show a different phase of the modulation amplitudes at large values of the WIMP mass compared to the standard velocity–independent cross–section, allowing to get a better fit of the DAMA data.

$$R \propto \int_{v_{min}} f(v)(v^2 - v^2_{min})$$

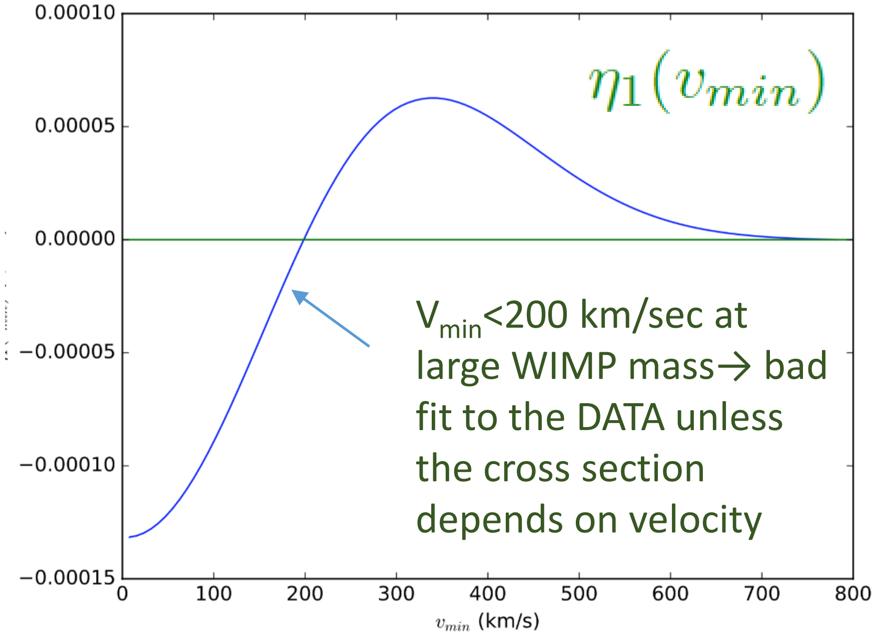

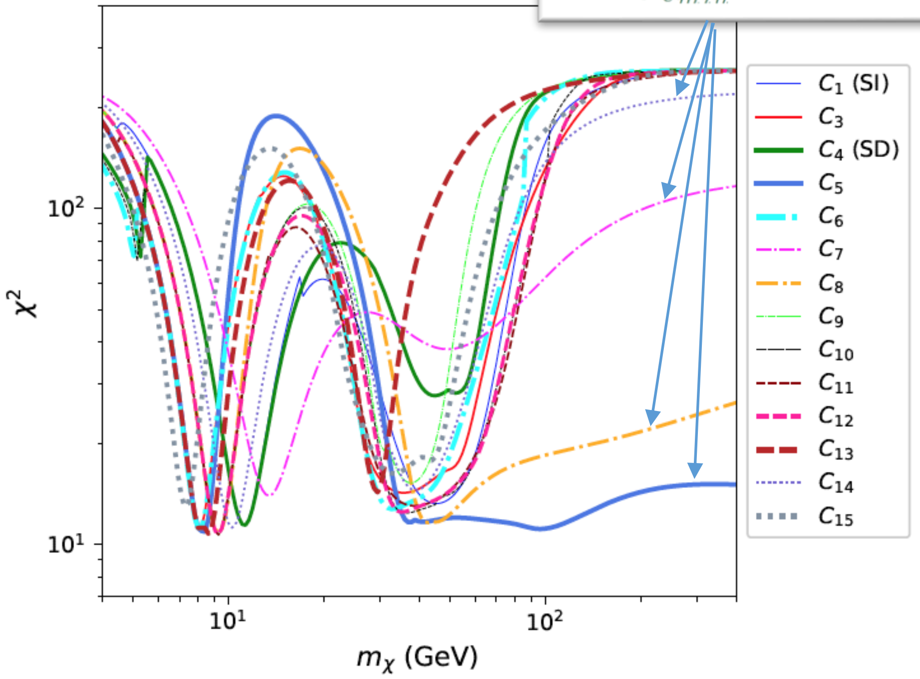

Sunghyun Kang, S.S., G. Tomar, J.H. Yoon, arXiv:1804.07528

c_j	$m_{\chi,\mathrm{min}}$ (GeV)	$r_{\chi,\mathrm{min}}$	σ (cm^2)	χ^2_{min}
c_1	11.17	-0.76	2.67e-38	11.38
	45.19	-0.66	1.60e-39	13.22
c_3	8.10	-3.14	2.27e-31	11.1
	35.68	-1.10	9.27e-35	14.23
c_4	11.22	1.71	2.95e-36	11.38
	44.71	-8.34	5.96e-36	27.7
c_5	8.34	-0.61	1.62e-29	10.83
	96.13	-5.74	3.63e-34	11.11
c_6	8.09	-7.20	5.05e-28	11.11
	32.9	-6.48	5.18e-31	12.74
c_7	13.41	-4.32	4.75e-30	13.94
	49.24	-0.65	1.35e-30	38.09
c_8	9.27	-0.84	8.67e-33	10.82
	42.33	-0.96	1.30e-34	11.6
c_9	9.3	4.36	8.29e-33	10.69
	37.51	-0.94	1.07e-33	15.23
c_{10}	9.29	3.25	4.74e-33	10.69
	36.81	0.09	2.25e-34	12.40
c_{11}	9.27	-0.67	1.15e-34	10.69
	38.51	-0.66	9.17e-37	13.02
c_{12}	9.26	-2.85	3.92e-34	10.69
	35.22	-1.93	2.40e-35	12.47
c_{13}	8.65	-0.26	1.21e-26	10.76
	29.42	0.10	5.88e-29	14.28
c_{14}	10.28	-0.59	2.61e-26	11.21
	38.88	-1.93	2.19e-27	14.48
c_{15}	7.32	-3.58	2.04e-27	12.91
	33.28	4.25	2.05e-33	16.26

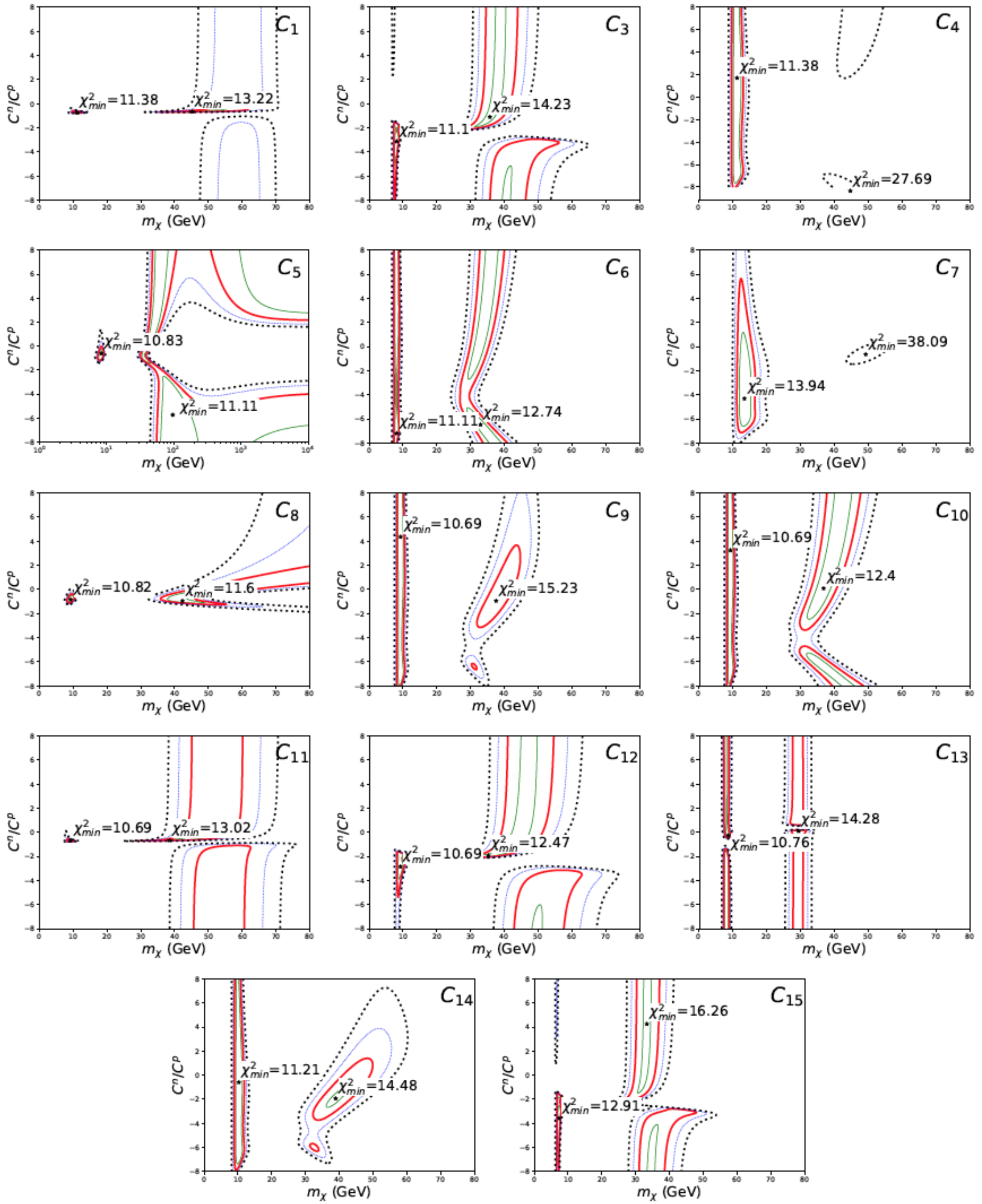

Sunghyun Kang, S.S., G. Tomar, J.H. Yoon, arXiv:1804.07528

- all models yield an acceptable χ^2
- in the worst case, i.e. c_7, $(\chi^2)_{min}$=13.74, with p–value $\simeq$ 0.25 with 14-3 degrees of freedom.
- for all of them with the exception of c_7 and c_{15} the absolute minimum of the χ^2 is below or equal to that corresponding the standard SI interaction c_1
- All bet-fit minima are in tension with the bounds from XENON1T and PICO60

DAMA best fit vs. Xenon1t and PICO60 exclusion plots

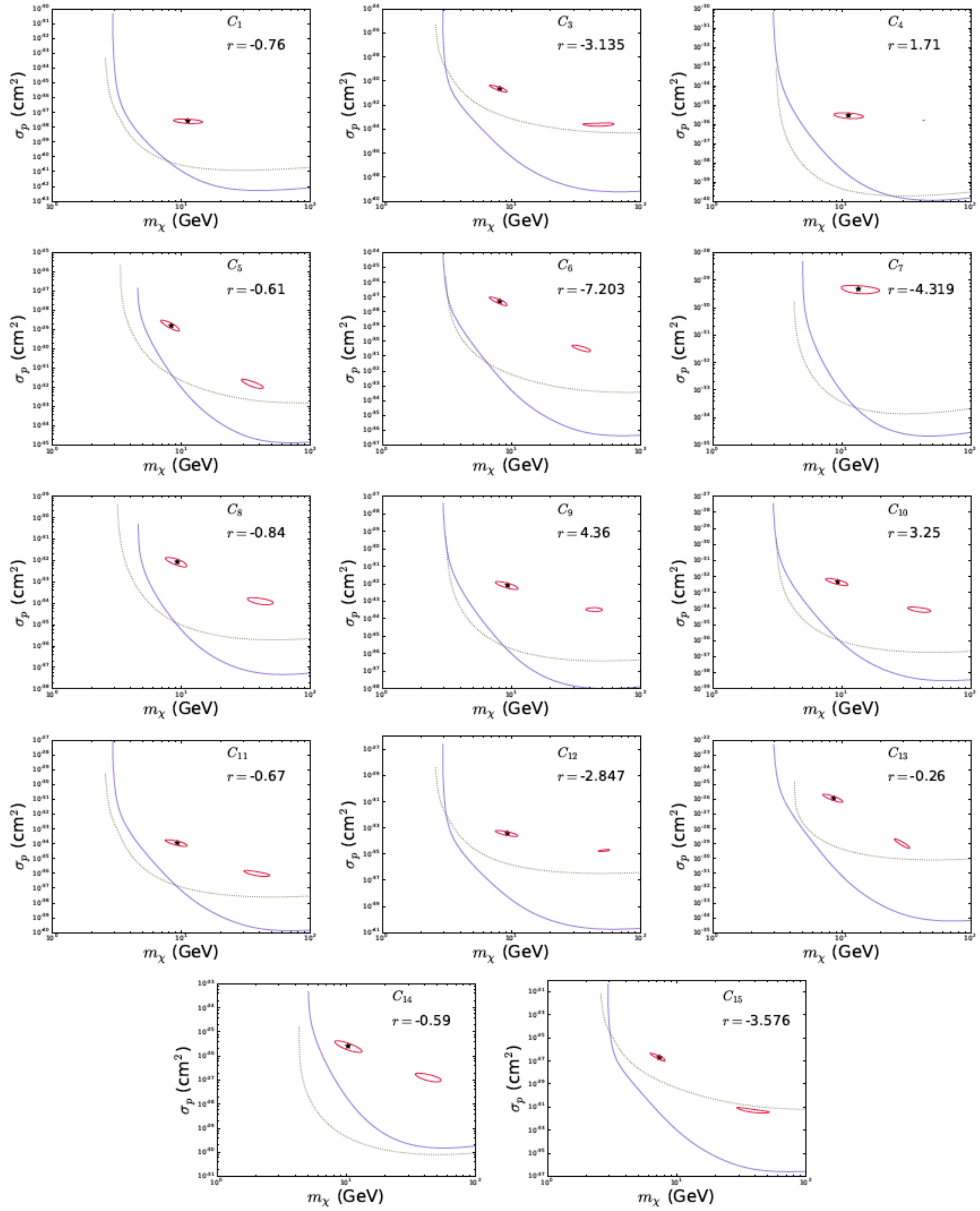

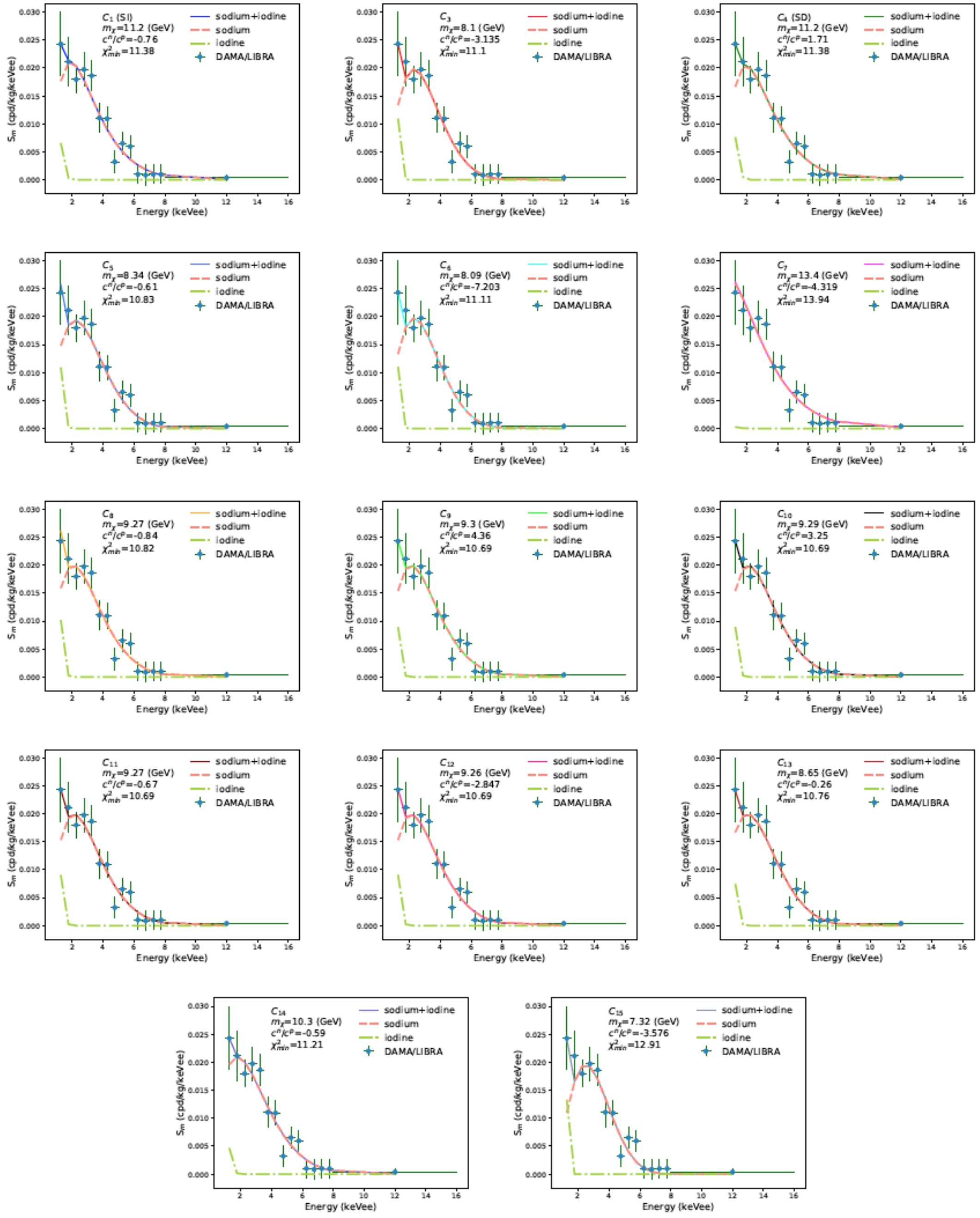

Sunghyun Kang, S.S., G. Tomar, J.H. Yoon, arXiv:1804.07528